

Chemical and mineralogical characteristics and origin of placer gold from fluvial deposits of Żeliszowski Creek (North Sudetic Basin, SW Poland)

Marcin KANIA¹

¹ "Poltegor-Institute" Opencast Mining Institute, Department of Geology, Parkowa 25, 51-616 Wrocław, Poland; ORCID: 0000-0002-6829-1663



Kania, M., 2023. Chemical and mineralogical characteristics and origin of placer gold from fluvial deposits of Żeliszowski Creek (North Sudetic Basin, SW Poland). *Geological Quarterly*, 67: 12, doi: 10.7306/gq.1682

Associate editor: Stanisław Mikulski

Chemical and mineralogical analyses of individual detrital gold grains collected from recent channel-fill deposits of Żeliszowski Creek, located between the towns of Lwówek Śląski and Bolesławiec, were made, together with determination of the Au-bearing mineral assemblages and indication of probable source areas. The analysed gold grains have admixtures of silver, mercury and copper. Numerous inclusions of ore minerals, mainly Cu, Hg selenides and Cu, Pb and Bi sulphides were found in the detrital gold grains. These minerals are characteristic of Permian, Au-bearing, red-bed successions in the region, and of quartz veins of the Kaczawa Metamorphic Complex. This supports the hypothesis of a polygenetic origin for the Lower Silesian alluvial gold-bearing deposits. The applied research methodology may be successfully used in polymetallic ore deposit prospecting more generally.

Key words: gold, Hg-amalgams, inclusions, placer deposits, North Sudetic Basin.

INTRODUCTION

Published mineralogical and chemical research into gold grains from Polish Cenozoic placer deposits has mainly been based on the particles' morphology (shape, size, roundness, surface textures) and on the mineralogical-petrographic composition of the Au-bearing sediments. This kind of research was undertaken by Grodzicki (1963, 1964a, b, 1966, 1969), who analysed gold-bearing deposits from the vicinity of Złotoryja, Mikołajowice-Wądroże Wielkie and Lwówek Śląski-Bolesławiec. Such research helped reveal the complex and prolonged genesis of the Sudetic gold-bearing deposits, which was initiated in the Paleogene and continued into the Holocene (Grodzicki, 1972, 1989, 1990, 1997, 1998, 2011).

Subsequent investigations, supplemented with chemical analyses of gold grains, led to revision of models of the origin of these Lower Silesian occurrences of detrital gold. So far, three main types of source area for the local detrital gold have been proposed:

1. red-bed type Permian Cu-polymetallic formation of the North Sudetic Basin (Urbański, 2010; Muszer, 2011; Oszczepalski et al., 2011; Wierchowicz and Zieliński, 2017; Kania, 2018);

2. quartz veins, mainly of the Kaczawa Metamorphic Complex (Kania, 2018; Wierchowicz et al., 2021) and granite gneiss of the Wądroże Massif (Grodzicki, 1966; Mikulski and Wierchowicz, 2013; Wierchowicz et al., 2018);
3. adjacent rocks of the Izera-Karkonosze Block (Grodzicki, 1963, 1969).

Furthermore, the local gold-bearing sands and pebbles may also be enriched in gold grains which originally crystallized in the primary Au-polymetallic deposits of Scandinavia (Jęczmyk and Krzemińska, 1996; Łuszczkiewicz and Muszer, 1999; Muszer, 2011). Some of the analysed gold grains were also described as probably anthropogenic-type particles (Wierchowicz, 2010, 2011; Muszer et al., 2016; Kania and Muszer, 2017).

This study combines detailed chemical analyses with exploration and identification of mineral microinclusions in gold grains, especially of ore minerals. Such methodology has not been previously applied to study of the Polish occurrences of the detrital gold, although it was applied by British geologists (Leake et al., 1995) investigating gold grains from Ecuador, the Malay Peninsula, Borneo and Zimbabwe. Microinclusions were also studied by Kelley et al. (2003), who used it in prospecting for Au-bearing hydrothermal veins in French Guyana.

The chemical composition of gold grains and mineralogy of the microinclusions can be used to determine conditions of gold mineralization and to indicate the type of primary deposit. Therefore, such research can be applied in prospecting for Au-polymetallic deposits, often rich in other scarce metals like silver, platinum, palladium, tellurium, bismuth and antimony.

* E-mail: kania.marcin@vp.pl

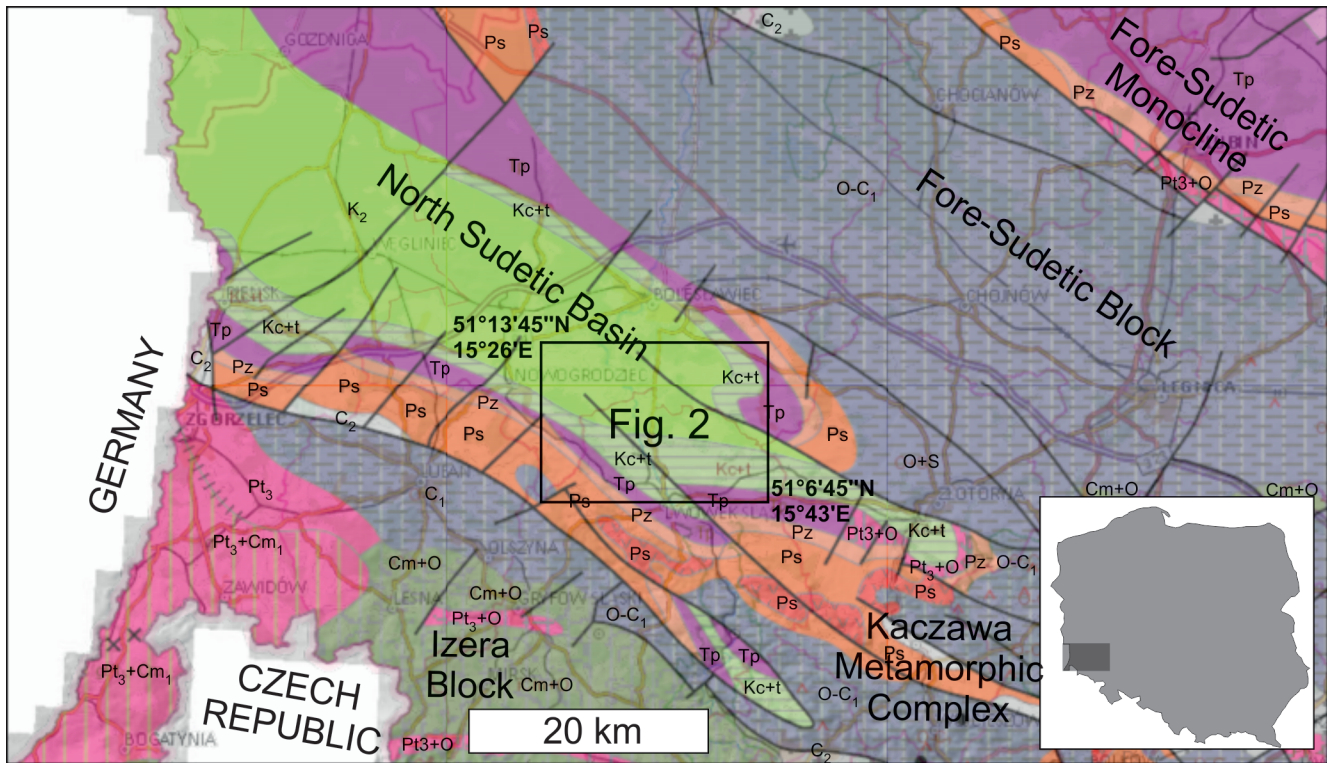


Fig. 1. Generalized geological map of the western part of the Lower Silesian Block without Cenozoic deposits (GeoLOG, modified)

Pt₃ – Upper Proterozoic, Cm₁ – Lower Cambrian, O – Ordovician, C₁ – Lower Carboniferous, C₂ – Upper Carboniferous, Ps – Rotliegend, Pz – Zechstein, Tp – Triassic (Bunter Sandstone), Kc+t – Cretaceous (Cenomanian and Turonian), K₂ – Upper Cretaceous

METHODS AND MATERIALS

The fieldwork included collecting samples of gold-bearing sediments and their simultaneous, preliminary concentration on-site. The sampling site constituted recent channel-fill deposits of Żeliszowski Creek, which is situated in an area of the gold-bearing sediments located between Lwówek Śląski and Bolesławiec towns (Figs. 1 and 2).

Sufficient gold grains were collected to allow detailed mineralogical and chemical studies, although determining the precise content of gold in the analysed alluvial sediments was not needed for this study. Samples were collected from places predisposed to concentration of heavy minerals, such as cracks in and spaces between boulders, cavities in the river bed and potholes. MKG devices were used in exploration of the river bed (Muszer et al., 2016; Kania, 2018; see also Kania, 2020 for further details of all the methodology used).

The concentrate samples were subsequently pan-washed, and the largest, macroscopically visible gold grains were recovered. The rest of the material was sifted on a 2 mm mesh sieve, then further prepared at the Department of Economic Geology of The Institute of Geological Sciences (University of Wrocław), first using a concentration table (Wilfrey type) with multiple re-processing. Diameters of isolated gold grains were measured using a binocular microscope. The heavy mineral concentrate obtained contained, other than native gold, grains of magnetite, ilmenite, haematite, martite, rutile, anatase, goethite, zircon, psilomelane, pyrolusite, minor cassiterite, monazite, garnet, apatite, scheelite, wolframite, pyrite and individual grains of chalcopyrite, bornite and covellite.

Polished sections were made from thus-isolated gold grains mounted in epoxy resin and subsequently were grinded and

polished. Struers materials were used: diamond discs (Piano type) for grinding, and cloths (MD-Dur, MD-Mol MD-Nap with dedicated solutions) for polishing.

The mineralogical and chemical composition was established both of the epoxy-embedded gold grains and of the microinclusions present within them.

Qualitative assessment of the grains' morphology was based on their cross-sections, to which a simplified DiLabio (1991) classification was applied. Here, a *pristine* class is represented by irregular, angular grains, while a *modified* class involves abraded grains with less well-marked features, that preserve their original irregular outlines but with curved or locally blunted edges. Grains subjected to a more intense abrasion are classified as *reshaped*, where original features are totally erased, to yield a regular, rounded shape.

To enable comparison of the gold grains' shape (rounding, irregularity) with their chemical and mineralogical composition (alloys, inclusions), an original procedure was additionally applied. This method is based on an outline development index (*K* index), defined as the relation of the length of a particular grain's outline to the length of circumference of a circle of an area equal to that of the analysed grain (Kania, 2020). A gold grain migrating in sediments is originally irregular, and becomes progressively rounded (Hérail et al., 1990; DiLabio, 1991; Loen, 1995; Wierchowicz, 2002; Kelley et al., 2003; Townley et al., 2003). Therefore, the relation between that grain's outline and the area of its cross-section steadily decreases (Kania, 2020). The *K* index is used in environmental sciences to calculate degrees of lakeshore development (Mizerski and Żukowski, 2001; Choiński, 2007). It can be adopted in mineralogical investigations to provide an objective evaluation of grain shape and to enable further comparative and statistical analyses.

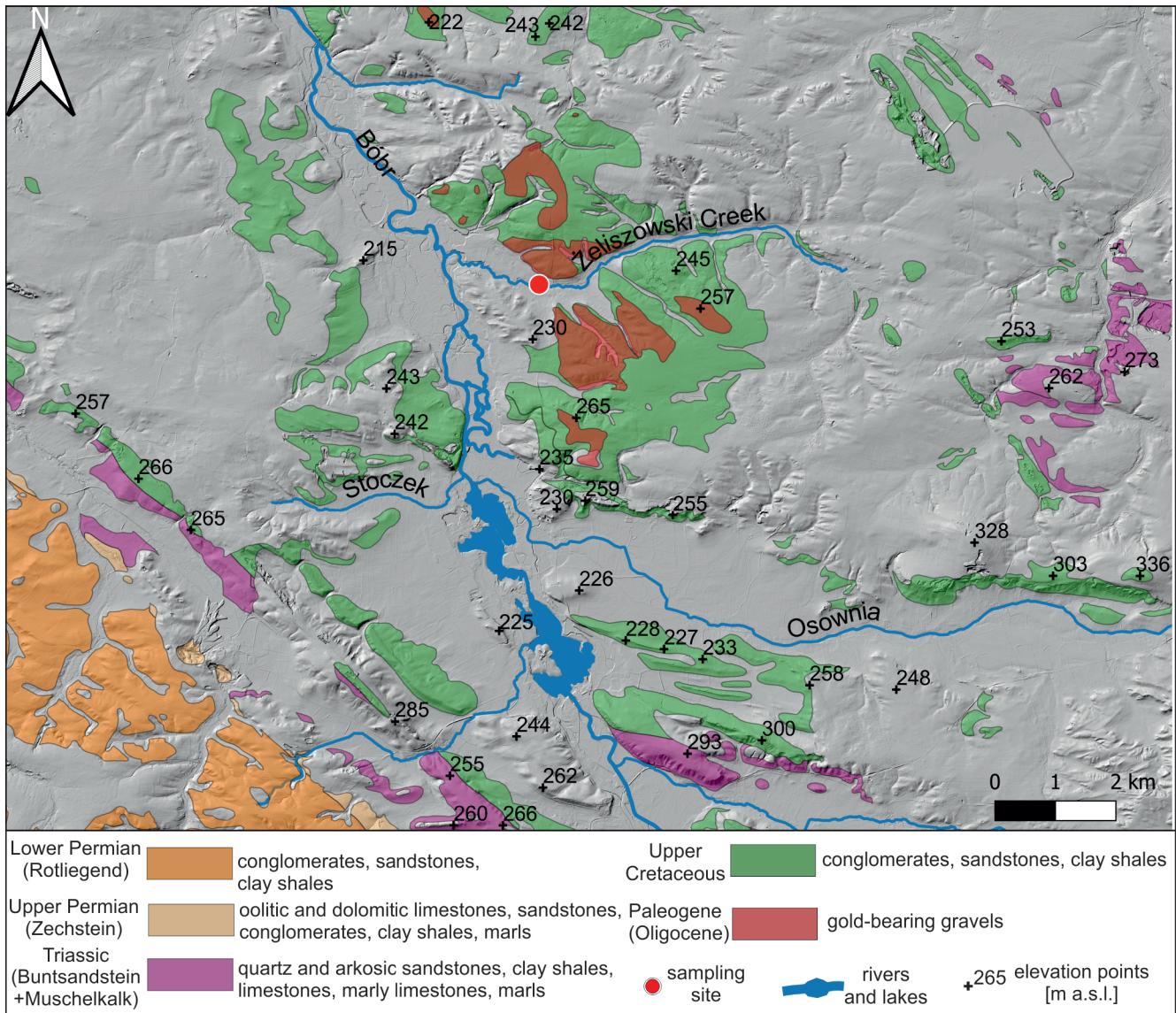


Fig. 2. Location of the sampling site, with simplified geological map and relief map (compiled after Grocholski, 1956; Milewicz, 1959; Grodzicki, 1969; Cymerman et al., 2009, 2012; Badura, 2013; Przybylski and Ichnatowicz, 2013)

The parameters required to calculate the *K* index were measured on BSE images of the gold grains, which are characterized by a high contrast between the particles and the background. To provide the measurements, *Surfer*® software was used. The outlines of the grains were defined in the form of polygons, with vertices located at an average distance of 77 nm.

To establish the phase composition of Au alloys and make preliminary identifications of mineral inclusions, the gold grains were observed in reflected light, using a universal *Nikon Eclipse LV100 POL* microscope. Observations of microinclusions finer than 10 μm were viable due to the use of a digital display coupled with the microscope. This set of devices enabled total magnification of up to 2500x.

The results of the diagnostic analyses in reflected light were always verified by means of EDS analyses, performed in the Laboratory of Electron Microscopy of the Wrocław Research Centre EIT+, using a FEI Quanta SEM with SDD Bruker XFlash EDS detectors. The methodology of the EDS analyses is described in detail in the [Appendix 1](#)

GEOLOGICAL SETTING

The area of the sampling site comprises un lithified deposits of the younger Cenozoic, from Oligocene to Holocene, as described below. These directly overlies the Mesozoic basement, which outcrops occur in the entire study area and is represented by various sedimentary rocks, from Permian to Cretaceous age, though lacking the Jurassic (Fig. 2).

The Mesozoic strata are underlain by the rocks of the Kaczawa Metamorphic Complex (KMC), also called the Złotoryja-Luboradz Unit (Baranowski et al., 1990) or the Kaczawa Schist-Greenstone Fold Belt (Żelaźniewicz et al., 2011). The Belt is composed of Paleozoic volcanic-sedimentary rocks, metamorphosed during the Variscan orogeny. This complex is bounded to the south-west by the Intra-Sudetic Fault, on the north, to the east by the Odra Dislocation Zone, and to the south by the Strzegom-Sobótka Granite Massif and the Ślęza Massif (Żelaźniewicz et al., 2011). The Belt extends to the west, beyond the Polish-German border, passing into the

Zgorzelec Phyllitic Fold Belt (Baranowski et al., 1990; Żelaźniewicz et al., 2011).

The KMC's evolution can be divided into two phases. Firstly, a pre-orogenic phase comprised initial (Cambrian-Ordovician) and mature (Silurian-Early Carboniferous) stages of oceanic crust formation. Secondly, there was the Variscan orogeny, when the Kaczawa Complex was deformed and altered, mainly in greenstone facies conditions (Furnes et al., 1994; Kryza, 2008).

The Variscan massif of the Kaczawa Complex was rebuilt during the Asturian phase, having undergone subsidence caused by NNE-SSW crustal stretching. In the western part of the stretched Variscan basement a sedimentary basin formed, the beginning of the North Sudetic Basin development (Baranowski et al., 1990; Karnkowski, 1999; Solecki, 2008). The basin is filled with unaltered, weakly tectonically disturbed sedimentary rocks dating from the Upper Carboniferous to the Upper Cretaceous. Sedimentation was brought to an end by the Laramian phase of the Alpine orogeny (Baranowski et al., 1990; Solecki, 2011).

Initially, in the Late Carboniferous, this Basin formed as a number of isolated fault troughs, filled by the products of erosion of the surrounding Variscan basement highs (Mastalerz and Raczyński, 1993; Solecki, 2008). Lithified clastic rocks comprise the sedimentary succession of the Upper Carboniferous-Lower Permian, in typical Rotliegend facies (Górecka, 1970; Baranowski et al., 1990; Solecki, 2008). During the orogenic movements of the Saalian phase renewed volcanism took place (Kozłowski and Parachoniak, 1967; Kiersnowski et al., 1995). Around the end of the Early Permian, the isolated fault troughs amalgamated into one, extensive sedimentary basin (Śliwiński et al., 2003).

Simultaneously, the late Carboniferous to early Permian witnessed the formation of the gold-bearing polymetallic quartz veins of the KMC, known mainly from the area of Radzimowice, Klecza-Radomice, Nielestno-Pilchowice, and Wielisław Złotyryjski. This hydrothermal mineralization was generated by local magmatic and volcanic phases, from the Bashkirian to the Artinskian (Mikulski, 2007a, c; Mikulski and Williams, 2014).

The Zechstein marine transgression resulted in a thick sequence of evaporitic deposits: metal-bearing marls, limestones, dolomites, anhydrites and sandstones (Baranowski et al., 1990; Solecki, 2008, 2011). The evaporites represent PZ1, PZ2 and PZ3 cyclothems (Raczyński, 1997; Śliwiński et al., 2003). Continental sediments of the Buntsandstein were deposited after the Zechstein regression. Marine sedimentation was re-established locally in part of the basin during the Middle Triassic and continued during the Late Triassic (Baranowski et al., 1990; Solecki, 2008, 2011). A further marine transgression occurred in the Cenomanian. As a result, a thick (~600 m) succession of sedimentary rocks accumulated (Baranowski et al., 1990). Towards the top of the Cretaceous succession, the deposits become finer, from Cenomanian conglomerates and sandstones, through Turonian and Coniacian sandstones, to Santonian continental clays and clayey sandstones, interbedded with brown coal seams (Milewicz, 1997; Solecki, 2008, 2011).

The Laramian tectonic activity around the Cretaceous-Paleogene boundary resulted in a change of a tectonic regime from tensional to compressive (Solecki, 1995, 2011). Inversion of the sedimentary basin led to development of the North Sudetic Basin. Regional NNE-SSW and NE-SW compression produced tectonic structures such as Wleń and Świerzawa troughs, and Leszczyna and Bolesławiec synclines (Baranowski et al., 1990; Solecki, 2011).

In the Cenozoic further subsidence and sedimentary deposition took place (Solecki, 2008). In the Oligocene gravels were deposited, and in the Miocene sands, gravels, clays and muds with a few lignite seams (Grocholski, 1956; Milewicz, 1959; Grodzicki, 1969, 1998), in the Miocene and Pliocene, kaolinic sands and gravels accumulated (Baranowski et al., 1990). Meanwhile, around the Paleogene-Neogene boundary, basaltic volcanism developed (Birkenmajer et al., 1977; Baranowski et al., 1990; Solecki, 2008). During the Pleistocene preglacial gravels and postglacial sediments of the South Polish (Mindel) and Mid-Polish (Riss) glaciations were deposited. The Pleistocene fluvio-glacial and alluvial, Holocene alluvial and anthropogenic deposits represent the youngest strata in the study area (Baranowski et al., 1990).

OCCURRENCE OF THE GOLD ORE MINERALIZATION IN THE STUDY AREA

In the study area and its vicinity, gold mineralization has been found in two settings. Locally, higher contents of Au occur in deposits that overlie epi-Variscan and Cenozoic strata; these result from a range of deposit-forming processes and include red-bed formations and un lithified gold-bearing sediments.

Gold mineralization is observed in stratabound, polymetallic, red-bed Permian strata across a large area of the North Sudetic Basin. Initial reports were limited to the „old copper district” mining area. The presence of Au traces within local Cu-bearing marls was shown by Konstantynowicz (1971), whilst Kucha et al. (1982) determined the content of gold in ore samples from the Konrad Mine as 4–10 ppm and indicated native silver as a main Au-bearing mineral (Oszczepalski et al., 2011). Gold prospecting in the North Sudetic Basin was expanded in the 1990s to the Rotliegend-Zechstein contact zone (Speczik and Wojciechowski, 1997; Wojciechowski, 1998, 2001, 2011; Oszczepalski et al., 2011).

Gold within the superficial sedimentary rocks of the Basin was best characterized around Nowy Kościół. Conglomeratic sandstone of Rotliegend age forms the lowest part of the local Cu-bearing succession, above which are Lower Zechstein carbonates (Basal Limestone), then mottled marl, Cu-bearing marl and Pb-bearing marl. These are overlain by karstic limestones with cavities filled with residual rock material: breccia, calcite and clay minerals. The Upper Zechstein clastic rocks, represented by metalliferous claystones and red sandstones, constitute the uppermost part of the profile (Romaniec and Janiec, 1957; Wojciechowski, 2001).

A two-part structure is characteristic of the polymetallic red-beds in Poland. The upper part of the metal-bearing profile is represented by sedimentary rocks formed in a reducing environment, and the lower part by oxidized deposits. According to Konstantynowicz (1965) and Skowronek (1968), the oxidized zone is of primary, synsedimentary origin, though more recent studies (Oszczepalski, 1989, 1999; Oszczepalski and Rydzewski, 1995, 1997; Piestrzyński et al., 1997, 2002; Speczik et al., 1997, 2003; Kucha and Przybyłowicz, 1999; Piestrzyński and Wodzicki, 2000; Oszczepalski et al., 2011) suggest that it has a post-sedimentary origin, with oxidation of rocks originally deposited in reducing conditions. Its characteristic red colour is due to hematite and Fe hydroxides as both grains and components of the cement (Rentzsch and Langer, 1963; Skowronek, 1968; Oszczepalski, 1989; Oszczepalski and Rydzewski, 1995 vide Oszczepalski et al., 2011). A transitional redox zone is characterized by a gradual colour change

from red to grey. Within this zone Fe oxides coexist with Cu-bearing sulphides: covellite, bornite, pyrite, chalcopyrite, often replaced by haematite.

The boundary between the oxidized and reduced zones is discordant in the strata of the North Sudetic Basin. The redox front is generally located within the marls, and locally involves the underlying Basal Limestone (Oszczepalski et al., 2011). The two-fold structure of the polymetallic succession is a consequence of its geochemical diversity: lead and silver are concentrated within the reduced zone, while deeper transition and oxidized zones are enriched in noble metals such as gold and PGEs. Au content in the oxidized zone is higher than that in the reduced and transition zones by one to nearly three orders (Oszczepalski et al., 2011).

Gold concentrations within the Rotliegend-Zechstein contact zone are much higher in the area of the Fore-Sudetic Monocline than in the North Sudetic Basin (Oszczepalski, 2007; Oszczepalski et al., 2011). Around Lwówek Śląski it reaches 18–40 ppb, while within Permian sedimentary rocks located along the southern edge of the Basin it does not exceed 100 ppb (Wojciechowski, 2001). There is a gold-bearing horizon, 0.6 m thick, located within Permian strata in the area of Nowy Kościół, enriched with Au up to 5.19 ppm. This higher concentration of gold coexists with a positive anomaly of Hg and F (up to 4.4 ppm and 0.12 wt.%, respectively). The local Au-bearing horizon comprises a sandy - argillaceous interval that separates conglomeratic sandstones from the Basal Limestone. The gold here was identified only by chemical methods, apparently in a form of adsorbate on Fe and Mn oxides and within pore spaces combined with haematite (Wojciechowski, 2001).

Cenozoic gold-bearing deposits constitute the second type of the gold ore in the study area, having one of the highest gold content amongst un lithified deposits in Poland. They occur as isolated layers, which extend from Bożejowice, Nowe Jaroszewice and Łaziska in the north to Dworek and Sobota in the south (Domaszewska, 1964; Grodzicki, 1969). Grodzicki (1998, 2011) distinguished four phases of their development. He indicated that the Oligocene-Neogene strata are the oldest that are genuinely Au-bearing and that the younger deposits (preglacial, Pleistocene and Holocene) were formed due to washing of the older ones. The deposits created during the first two phases are characterized by a significantly higher amount of native gold, of up to 15 g/t in places (Quiring, 1913, 1914; Schumacher, 1924; Grodzicki, 1963, 1969).

The Oligocene-Neogene phase occurred under warm and humid climatic conditions. The gold-bearing source rocks underwent intense mechanical erosion, to form eluvial - deluvial covers of gravel and sand. The gravels and sands contain impurities and interlayers of argillaceous - loamy material with higher Au concentrations (Grodzicki, 1966, 1998). According to Grodzicki (1972, 1998) the Oligocene-Neogene phase is represented by part of the alluvial white and yellow quartz gravels and sands occurring north of Lwówek Śląski. In the area of Włodzice these >4 m-thick deposits directly overlie lithified basement composed of Upper Cretaceous sandstones (Grodzicki, 1969). The gold grains appear in the form of yellow scales, flakes and wires with a red coloration, mostly <0.5 mm in size (Grodzicki, 1969, 1998).

The second, preglacial phase includes the Upper Pliocene and the Lower Pleistocene. Alpine (Rodanian and Wallachian) orogenic tectonic processes and climate cooling intensified fluvial erosion. Partial washout of older gold-bearing deposits occurred east of Lwówek Śląski and north-east of Złotoryja. The redeposited sediments are characterized by considerable petrographic and mineralogical variety, with co-existence of pebbles and minerals of varying resistance to abrasion and

chemical weathering. The content of less weathering-resistant minerals is higher than in the Oligocene-Neogene deposits, while native gold occurs in trace amounts (Grodzicki, 1963, 1972, 1998).

Pleistocene climate cooling led to suppression of chemical weathering of the gold-bearing source rocks. With reduced weathering, there was impoverishment of the Pleistocene deposits in gold. Higher concentrations of native gold occur only within the postglacial deposits of the South Polish glaciation (Mindel), enriched via reworking of older Au-bearing deposits (Grodzicki, 1963, 1998).

According to Grodzicki (1963) Holocene gold-bearing sediments are composed of both Au grains redeposited from older deposits and deposited directly from currently eroded source rocks. The average content of native gold within the contemporary alluvium of the Kaczawa river basin is 0.02 g/t. The main mineral components of the Holocene deposits of the Złotoryja area are quartz grains, porphyry and quartzite clasts, and minor amounts of crystalline schist, phyllite, amphibolite and granite. The heavy mineral composition is dominated by epidote, magnetite, ilmenite, leucoxene, zircon and rutile, minor amounts of garnet, kyanite, hornblende, tourmaline and haematite. Grains of anatase, sphene, topaz, chrysoberyl and corundum coexist with native gold in trace amounts (Grodzicki, 1963).

RESULTS

MORPHOLOGY AND CHEMICAL COMPOSITION

Fourteen gold grains were selected for detailed mineralogical-chemical study. The gold grains from the Żeliszowski Potok sediments are mostly of modified type *sensu* DiLabio (1991). They are characterized by dendritic, partially rounded shapes (grains Z-1, Z-6, Z-11, Z-12), and numerous overgrowths and voids after rock-forming minerals (Z-2, Z-3, Z-13). The Z-8 gold grain is characterized by the highest *K* index value with its irregular, dendritic shape, typical of pristine grains. Single, discoidal reshaped grains with elongated outlines (Z-9, Z-10) also occur (Fig. 3). The *K* index values vary from 1.13 to 5.83, although most common are particles with the index value ranges of 1–2 and 2–3 (average value 2.85). Even within the group of grains with rounded corners suggesting heavy abrasion (such as Z-4, Z-5 and Z-11), the *K* indices are varied and reflect the presence of the discrete forms of grain morphology, such as cavities, bends, folds, cracks, dissolution pits and canals.

The grains analysed vary in circumference from 15 to almost 800 µm, with an average diameter of 295 µm. Grains of 100–200 µm in size occur most frequently. Microinclusions of rock-forming minerals (mainly clay minerals and quartz, exceptionally feldspars, zircon and calcite) were found inside most examined grains, and microinclusions of ore minerals (sulphides and selenides) only in two of them.

Silver, copper and mercury were present within the gold grains. Silver is the most common admixture, its content not exceeding the first metastable phase (22–38 wt.%), which formed i.a. a multiphase Z-8 amalgam (Fig. 4). In structure and elemental distribution this 150 µm particle is similar to the *bimodal* gold grains distinguished by Wierchowicz and Zieliński (2017). The core of the grain is composed of a metastable phase, while the rim is composed of a native gold phase, often porous; the contact between the phases is always sharp. Mercury is limited to the metastable phase. Although grain Z-8 is devoid of ore mineral microinclusions, its angular shape and multiphase structure are features indicating the natural origin of this type of amalgam (Kania and Muszer, 2017).

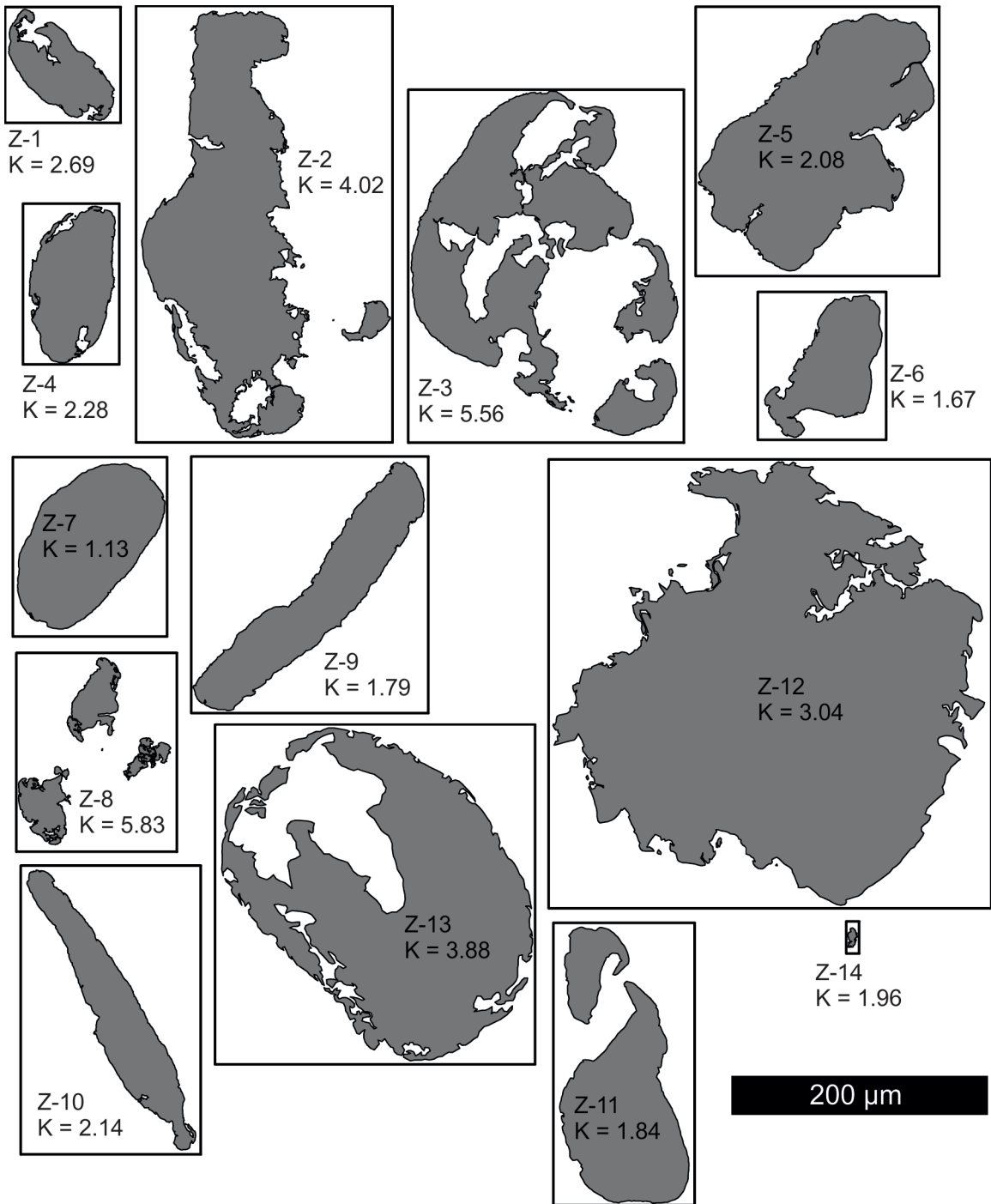


Fig. 3. Outlines of the gold grains prepared for the detailed analyses, relative to the calculated K index values

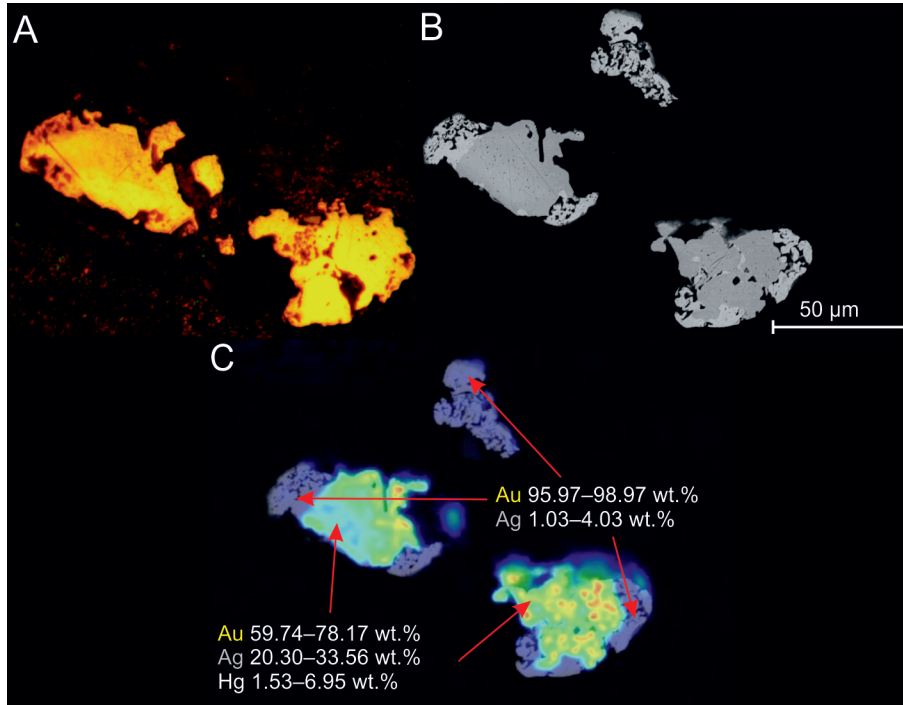


Fig. 4. The Z-8 multiphase amalgam

A – image in reflected light; **B** – BSE image; **C** – silver distribution: green, yellow, up to red colours indicate the higher concentration of Ag

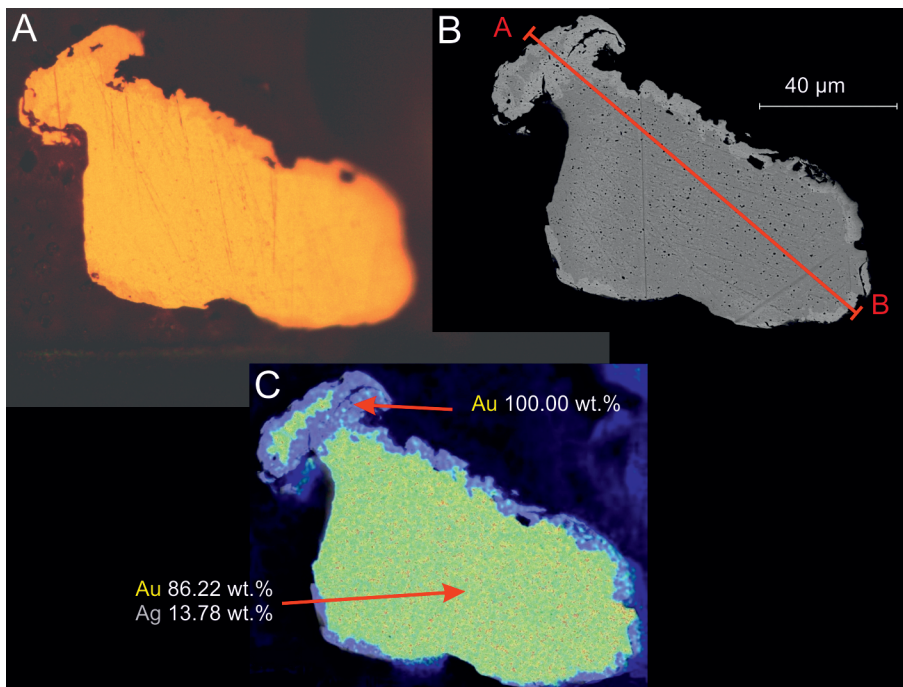


Fig. 5. The single-phase Z-6 gold grain with edges impoverished in silver

A – image in reflected light; **B** – BSE image with the marked profile of the linear analyses (results in Fig. 6); **C** – silver distribution: green colour indicates the higher concentration of Ag

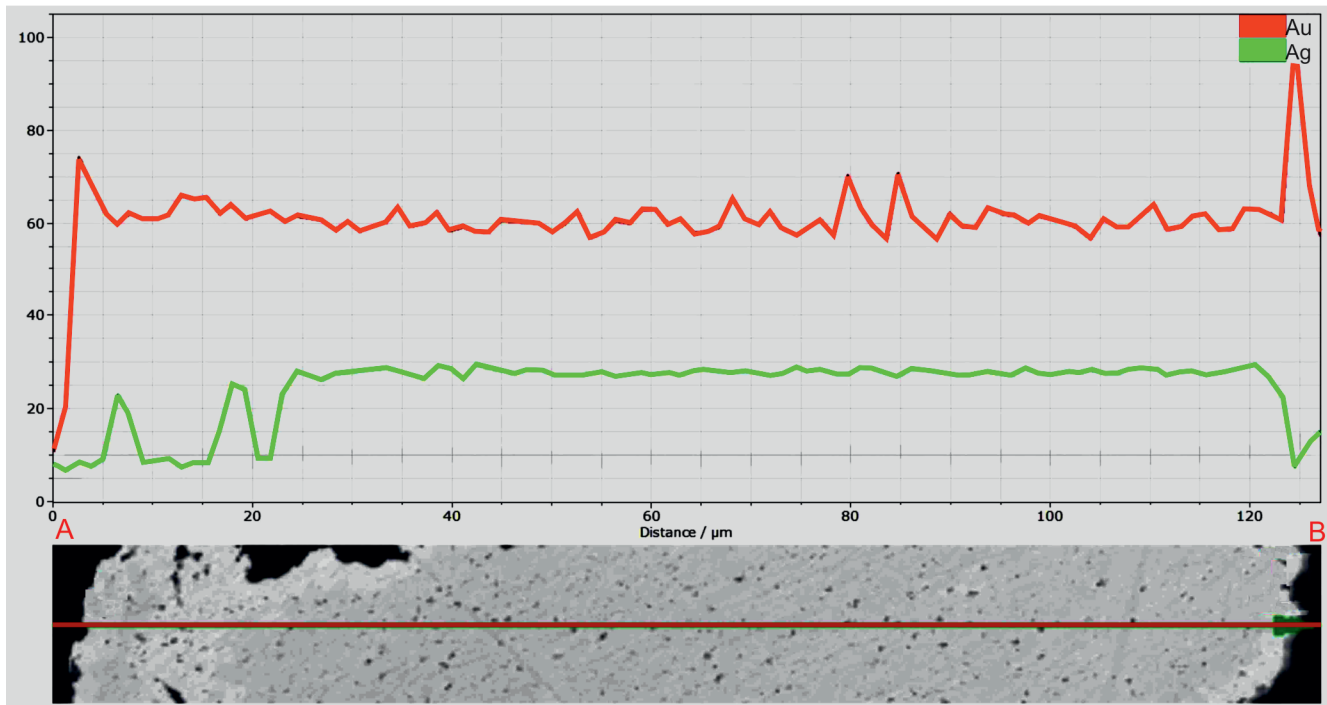


Fig. 6. Linear analyses of the Au and Ag contents within the Z-6 gold grain

Location of the profile in [Figure 5](#)

Among the examined gold particles there are no rounded grains with well-developed spongy structure, which are the characteristic features of anthropogenic amalgams ([Leake et al., 1995](#); [Kelley et al., 2003](#); [Muszer et al., 2016](#); [Kania and Muszer, 2017](#)).

The distribution of silver within the most examined grains is often variable, though the phase compositions is stable, with Ag contents not exceeding 15 wt.% in any of the points analysed. Enrichments in silver are present both in central and outer parts of the grains, locally marked by distinct boundaries ([Fig. 5](#)).

The copper content within the gold grains does not generally exceed 1 wt.%, though in one case it reaches 22.42 wt.%. The gold significantly enriched in copper (<17.44 wt.%) occurs within the Z-2 gold grain as individual rounded phases, finer than 1 μm. The phase locations have no spatial relation to the silver distribution ([Fig. 7](#)) and are distinguished by their characteristic reddish/pinkish colour ([Fig. 8](#)). Their Au:Cu ratio varies between 1:1 and 1.5:1 and corresponds to the tetraaricupride phase CuAu. No microinclusions of ore minerals were identified within the Z-2 grain.

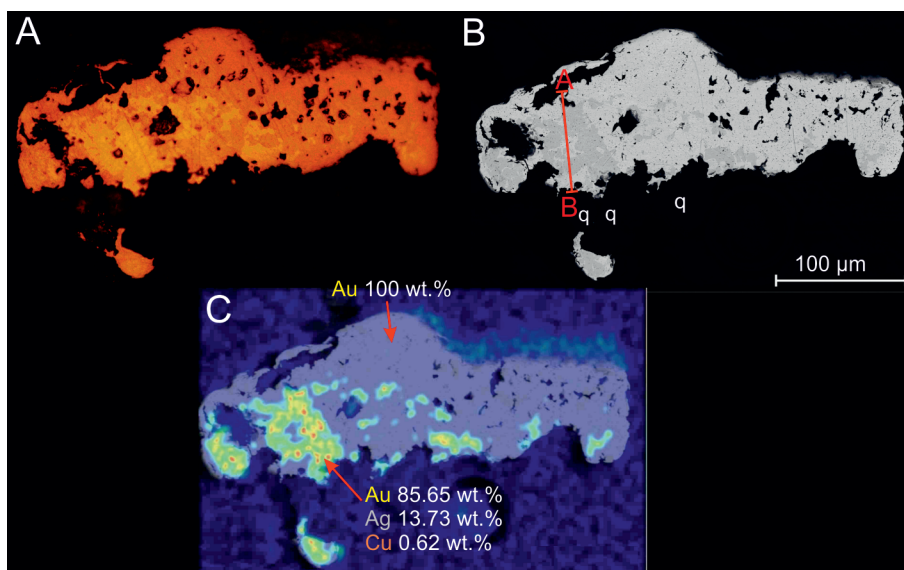


Fig. 7. The cupriferous Z-2 gold grain

A – image in reflected light; B – BSE image with the marked profile of the linear analyses (results in [Fig. 9](#)), q - quartz; C – silver distribution: green, yellow, up to red colours indicate the higher concentration of Ag

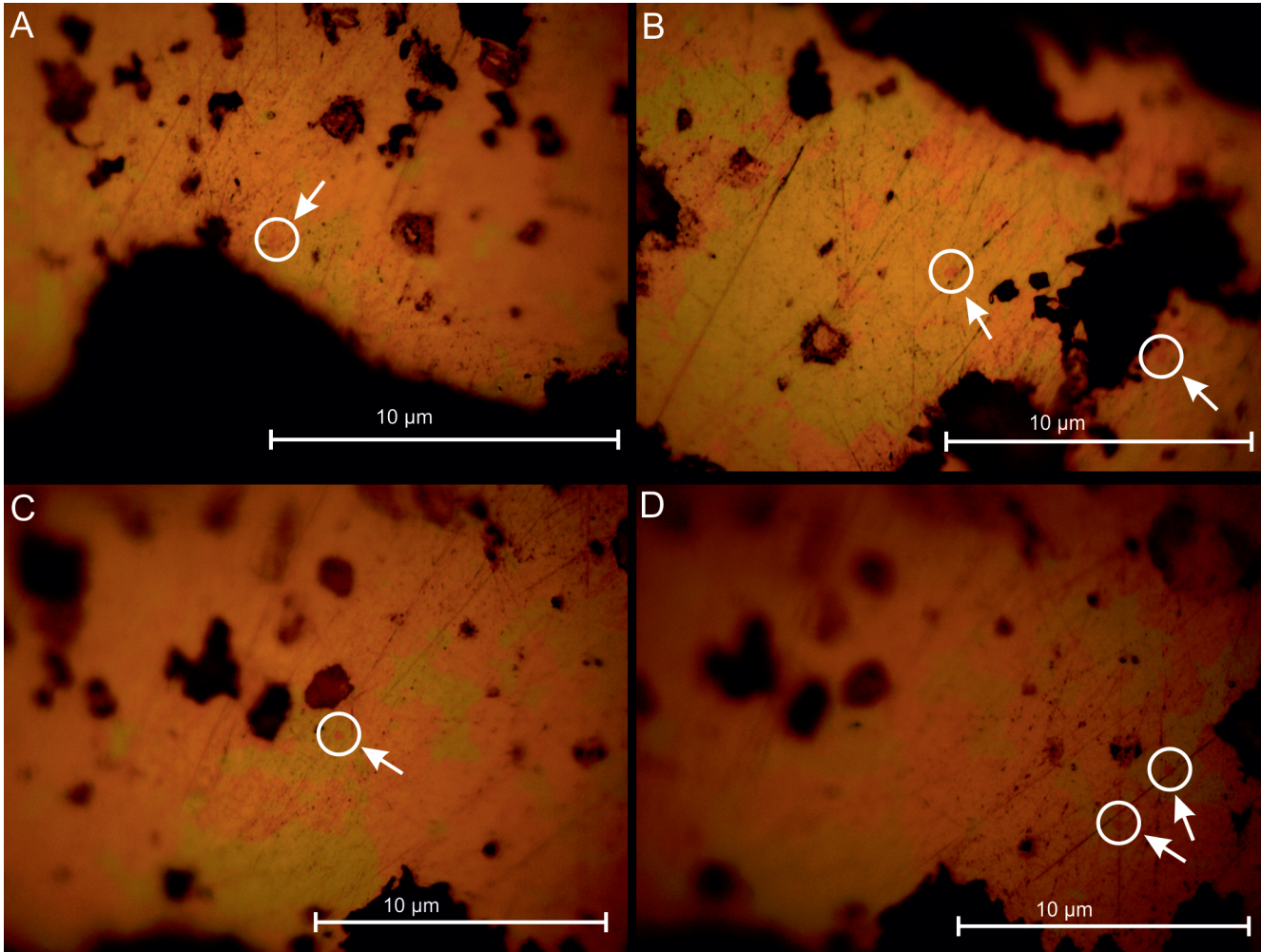


Fig. 8. Phases of cupriferous gold of tetraauricupride composition within the Z-2 gold grain, reflected light

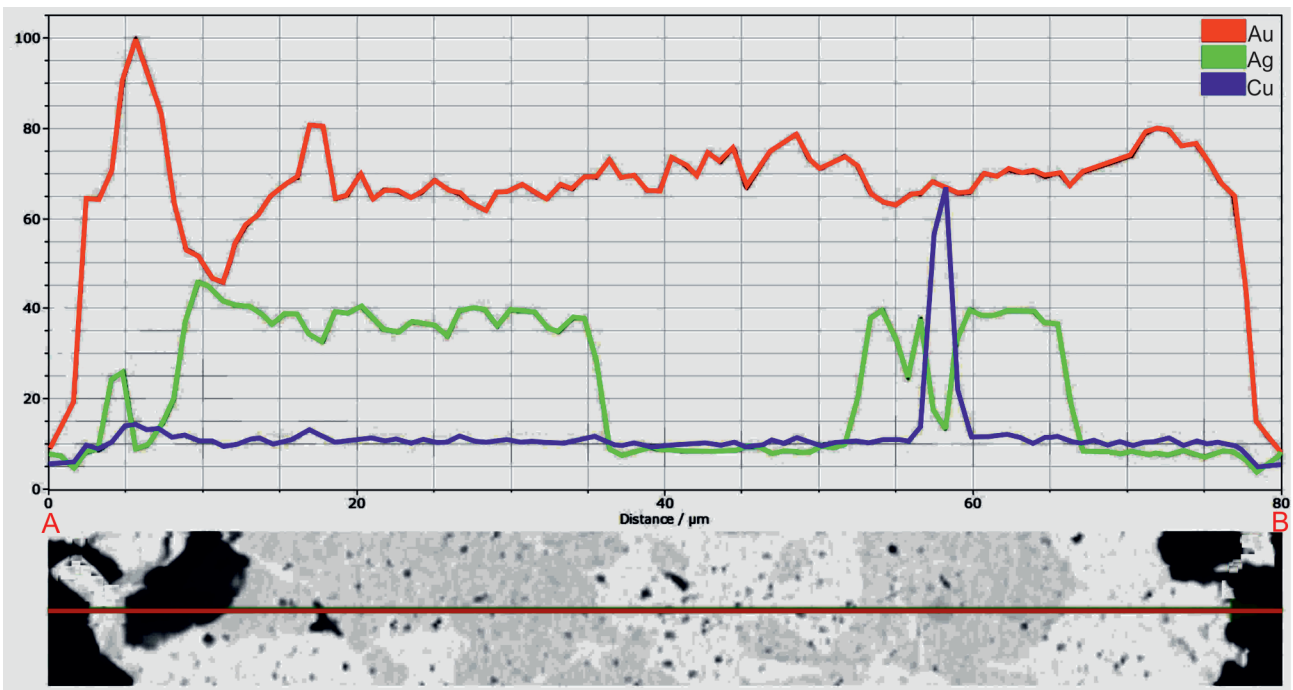


Fig. 9. Linear analyses of Au, Ag and Cu contents within the Z-2 gold grain

Location of the profile in [Figure 7](#)

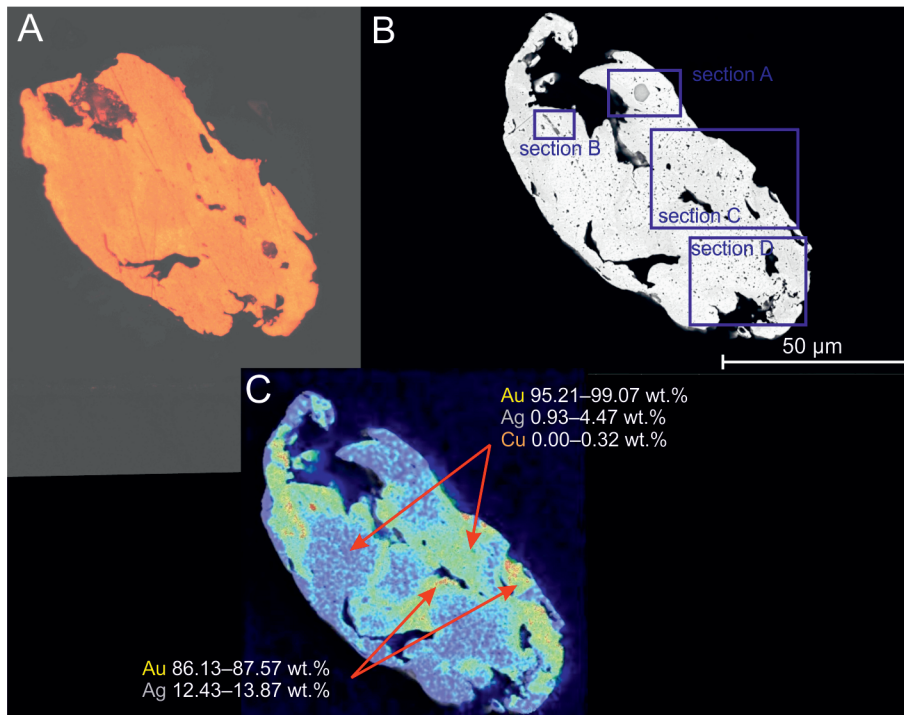


Fig. 10. The ore-bearing Z-1 gold grain

A – image in reflected light; B – BSE image, marked location of the sections; C – silver distribution: green, yellow, up to red colours indicate the higher concentration of Ag

MICROINCLUSIONS

Ore mineral inclusions were identified in the two of the gold grains, and one further grain with a polycrystalline, granular aggregate was found. The ore-bearing gold grains are composed of the homogeneous native gold phase.

The Z-1 gold grain previously described by [Kania and Muszer \(2017\)](#) remains the richest in microinclusions among all the grains examined ([Fig. 10](#)). It has a diameter of 105 µm. Silver occurs in amounts up to 13.87 wt.%. Numerous fine microinclusions appear throughout the grain. They include

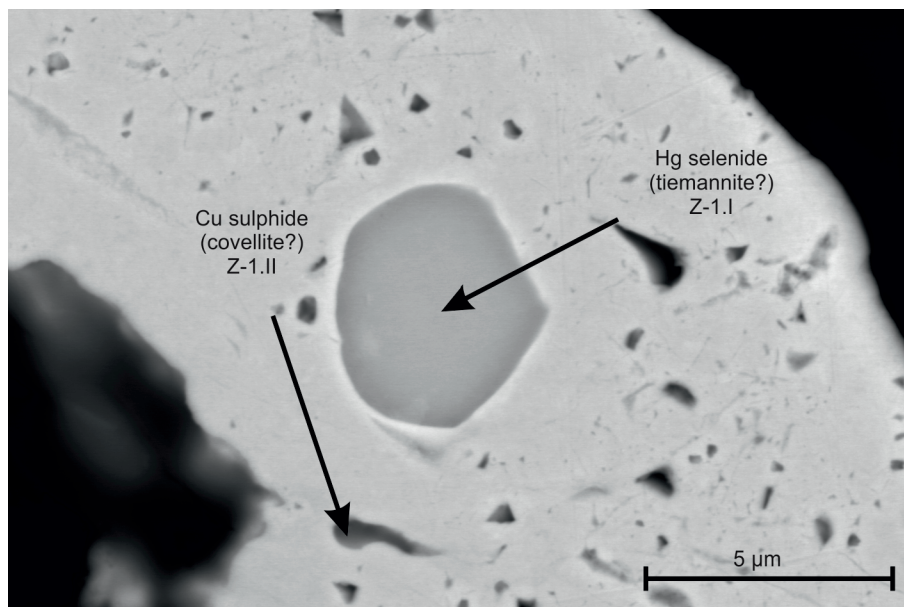


Fig. 11. Enlargement of section A – inclusions of tiemannite and covellite compositions within the Z-1 gold grain

BSE image with the marked location of the analysed points (the results in the [Appendix 1](#)), the location of the zoomed section in [Figure 10](#)

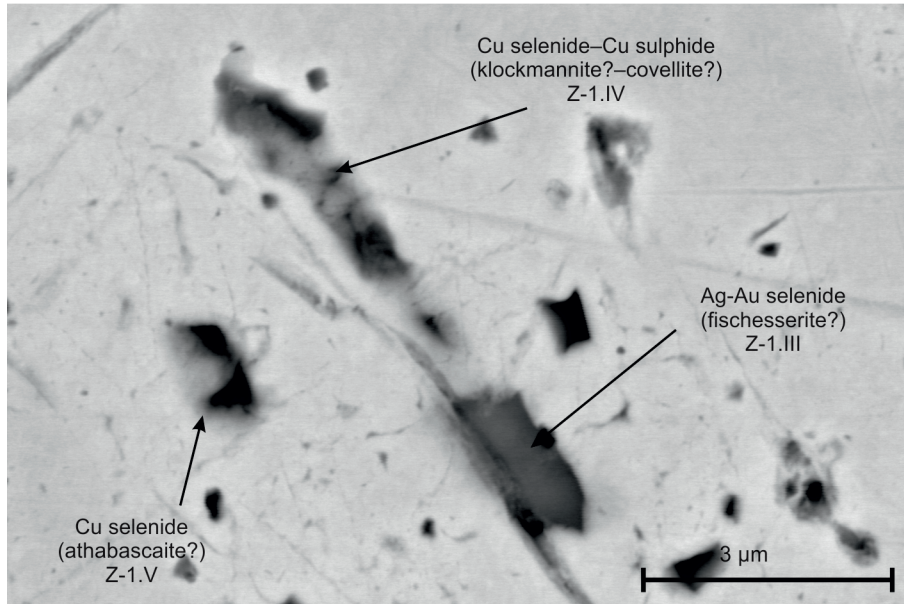


Fig. 12. Enlargement of section B – inclusions of selenide composition within the Z-1 gold grain

BSE image with the marked location of the analysed points (the results in the [Appendix 1](#)), the location of the zoomed section in [Figure 10](#)

selenides of tiemannite composition, several Cu selenides of klockmannite-athabaskaite-umangite series compositions, a single Ag-Cu-Au selenide of fischesserite composition, covellite and a diphase inclusion of klockmannite-covellite composition. Hipautomorphic tiemannite, a xenomorphic overgrowth of klockmannite and covellite and automorphic athabaskaite and fischesserite form the largest inclusions with diameters of >1 µm, up to 5 µm ([Figs. 11 and 12](#)). The remaining ore minerals identified form xenomorphic microinclusions ([Fig. 13](#)). The

grain is composed of the native gold phase with additions of silver and copper of up to 13.87 and 0.32 wt.%, respectively ([Fig. 10](#)). Repeated point analyses, performed after the re-polishing of the grain, excluded the presence of mercury within the gold alloy ([Kania and Muszer, 2017](#)). Its presence was most likely connected with subsurface, imperceptible microinclusions of Hg-bearing ore minerals such as the Hg selenide (tiemannite?) described.

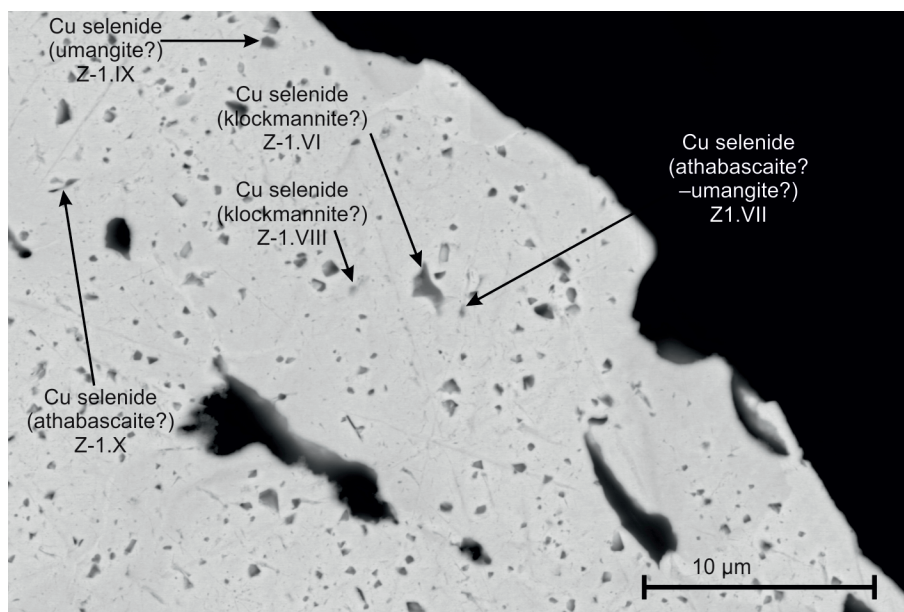


Fig. 13. Enlargement of section C – inclusions of selenide composition within the Z-1 gold grain

BSE image with the marked location of the analysed points (the results in the [Appendix 1](#)), the location of the zoomed section in [Figure 10](#)

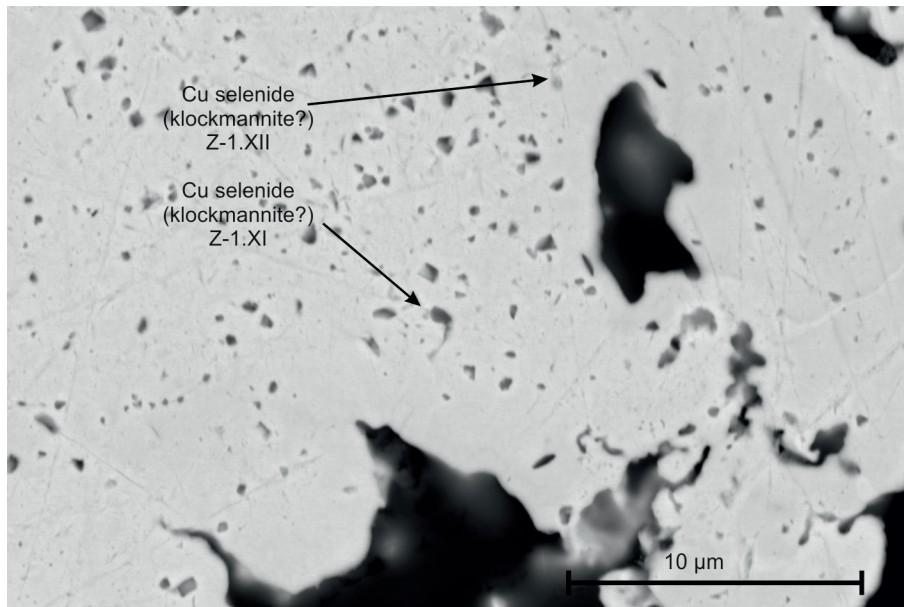


Fig. 14. Enlargement of section D – inclusions of selenide composition within the Z-1 gold grain

BSE image with the marked location of the analysed points (the results in the [Appendix 1](#)), the location of the zoomed section in [Figure 10](#)

Z-11, the other ore-bearing gold grain ([Fig. 15](#)), is 450 μm in diameter and contains two overgrowths of automorphic bismuthinite with hipautomorphic covellite composition. The first of the bismuthinites is cut along the short axis ([Fig. 16](#)), and the second along the long axis of the crystal reaching a length of 4 μm ([Fig. 17](#)). The covellites are up to 1 μm in size. In addition, a hipautomorphic, 2 μm galena particle occurs within the Z-11 gold grain ([Fig. 18](#)).

A unique polycrystalline aggregate was found inside the 300-micrometre Z-3 gold grain ([Fig. 19](#)), co-created by numerous quartz grains measuring from 5 to 80 μm in diameter, alkali Na-K feldspars (up to 30 μm) and a single zircon grain. All these

rock-forming minerals are angular and free from visible signs of the surface abrasion. They are cemented by Fe hydroxides characterized by their rusty colour, visible in reflected light ([Fig. 19A](#)). These iron compounds constitute a relict of primary ore mineralization.

DISCUSSION

Both the chemical composition of the gold grains and the mineralogical composition of the microinclusions indicate a likely connection between the detrital gold occurrences of the

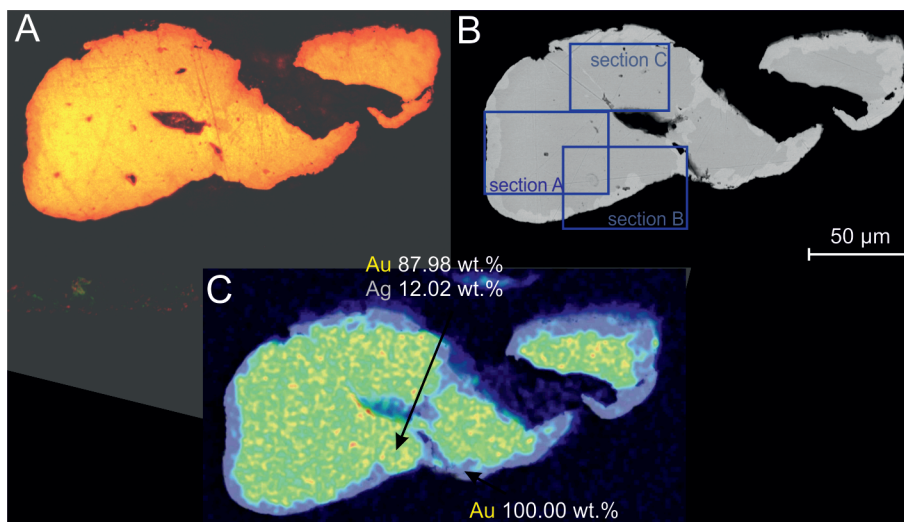


Fig. 15. The ore-bearing Z-11 gold grain

A – image in reflected light; B – BSE image, the marked sections (zoomed sections in [Figs. 16–18](#)); C – silver distribution: green, yellow, up to red colours indicate the higher concentration of Ag

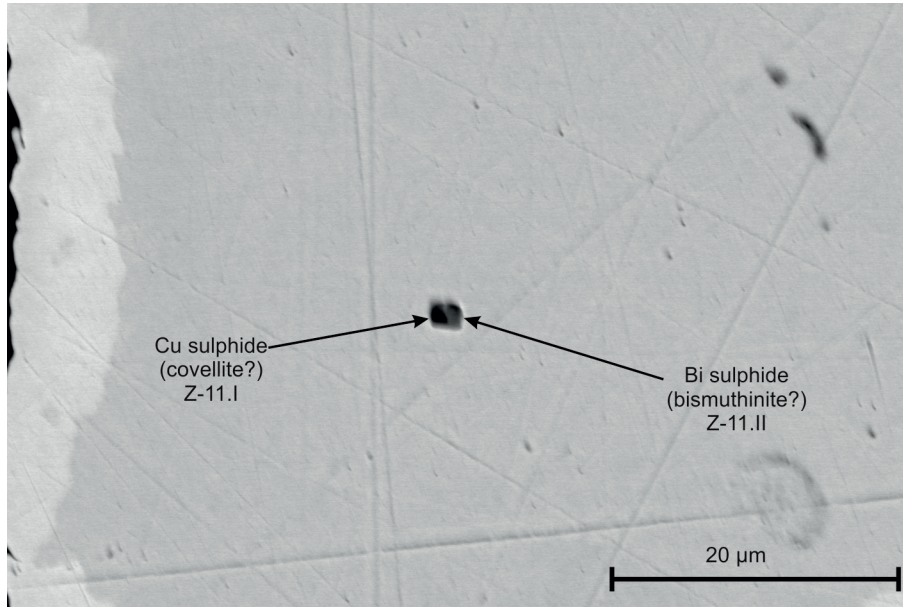


Fig. 16. Section A – overgrowth of Cu and Bi sulphides within the Z-11 gold grain

BSE image with the marked location of the analysed points (the results in the [Appendix 1](#)), the location of the zoomed section in [Figure 15](#)

Kaczawa Foothills, the Au-polymetallic mineralization of the local Permian sedimentary rocks and the quartz veins of the Kaczawa Metamorphic Complex. Evidence for this comprises the coexistence of multiphase amalgams and copper-bearing gold grains, the presence of the Cu- and Hg-bearing selenide inclusions, and Cu-Pb-Bi sulphides.

The multiphase amalgams from the Żeliszowski and the Jamna Creeks ([Kania and Muszer, 2017](#); [Kania, 2018](#)) and the *bimodal* gold particles from the vicinity of Grodziec ([Wierchowicz and Zieliński, 2017](#)) are characterized by a simi-

lar structure and phase composition. The presence of mercury as well as the Z-8 grain's pristine shape are indicators of its brief transport. According to [Wierchowicz and Zieliński \(2017\)](#), mercury occurrence within gold minerals indicates a late, epithermal stage of their crystallization in the source rock. The Au-Ag amalgams were formed by the recrystallization of the original Au-Ag-Pd minerals under the influence of low-temperature Hg-bearing solutions.

Moreover, the multiphase amalgams obtained from the Jamna ([Kania, 2018](#)) and Żeliszowski Creeks reveal a similar

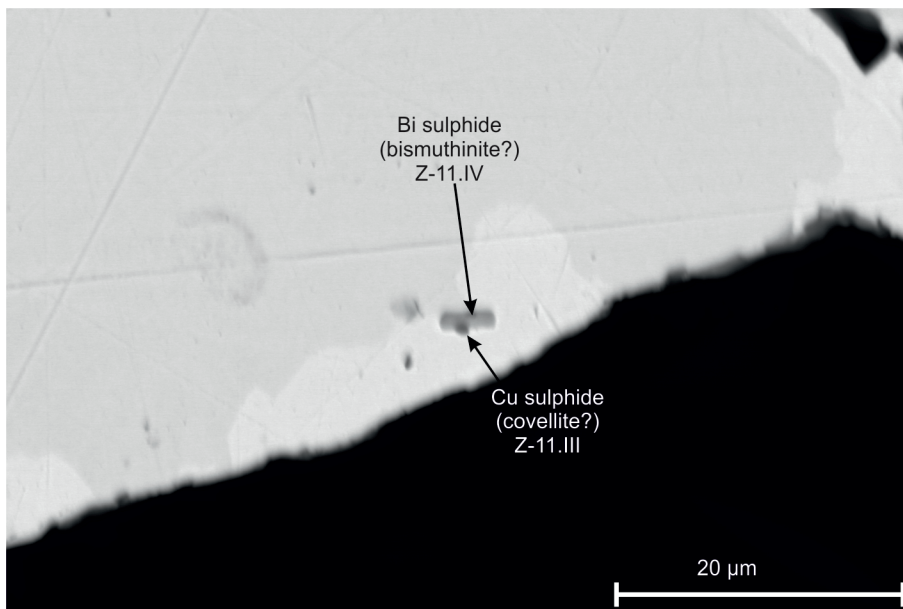


Fig. 17. Section B – overgrowth of Cu and Bi sulphides within the Z-11 gold grain

BSE image with the marked location of the analysed points (the results in the [Appendix 1](#)), the location of the zoomed section in [Figure 15](#)

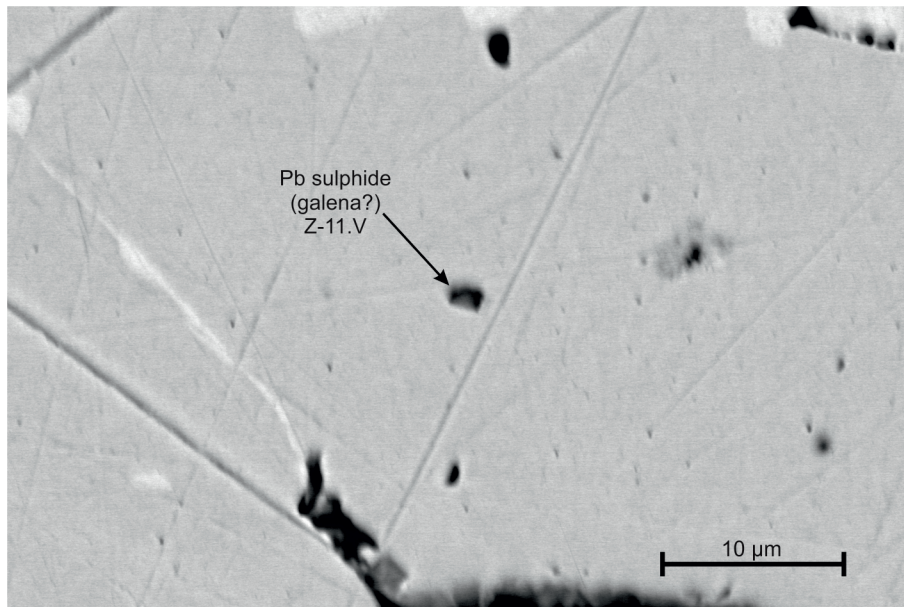


Fig. 18. Section C – an inclusion of Pb sulphide (galena?) within the Z-1 gold grain

BSE image with the marked location of the analysed point (the results in the [Appendix 1](#)), the location of the zoomed section in [Figure 15](#)

structure and phase composition to the Hg-bearing electrum from the cupriferous Zechstein Boundary Dolomite identified in the Polkowice Mine. Within this electrum, described by [Piestrzyński et al. \(2002\)](#) and [Piestrzyński and Pieczonka \(1998\)](#), the first occurrence of rare tetraauricupride CuAu in Poland was identified. Numerous fine phases with an atomic Cu:Ag ratio close to one have been also found within the Z-2 gold grain from Żeliszowski Creek ([Fig. 8](#)), which may be the second occurrence of tetraauricupride in Poland.

The red to pink shade of the gold grains, characteristic of Au-Cu alloys of both natural and artificial origin ([Saeger and Rodies, 1977](#); [Cretu and Lingen, 1999](#)), should be also attributed to the Cu-polymetallic mineralization in the Permian succession. Numerous detrital occurrences of reddish and pinkish gold grains have been described in the vicinity of Lwówek Śląski, Bolesławiec and Złotyryja ([Grodzicki, 1963, 1969](#); [Muszer, 2011](#)).

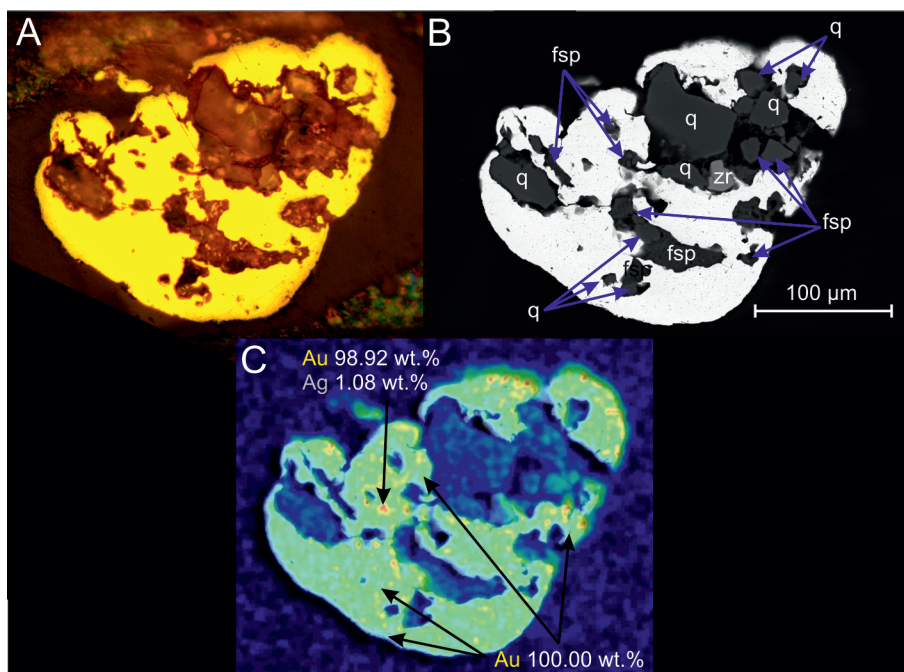


Fig. 19. The Z-3 gold grain with a polycrystalline aggregate of rock-forming minerals

A – image in reflected light; **B** – BSE image: q – quartz, fsp – Na-K-Ca feldspars, zr – zircon; **C** – silver distribution: green, yellow, up to red colours indicate the higher concentration of Ag

The mineral composition results obtained for the microinclusions indicate additional source areas for the detrital gold analysed from the Permian red beds. The inclusions are represented by an epithermal assemblage of ore minerals (especially selenides), previously identified in heavy mineral concentrates from Holocene alluvial deposits from around Lwówek Śląski (Muszer, 2011). Scarce selenides and Se-bearing sulphides from the Lower Silesian copper deposits were described by Kanasiewicz (1964, 1966, 1967), whilst Pieczonka et al. (2008) and Pieczonka and Piestrzyński (2011, 2015) characterized various selenides occurring in the secondarily oxidized parts of the Permian Cu-polymetallic deposits.

However, the origin of the detrital gold present in the Żeliszowki Creek sediments seems not as clear as in the case of the gold grains from the Grodziec area (Wierchowicz and Zieliński, 2017) and Jamna Creek (Kania, 2018). Nowadays there are no outcrops of the metalliferous Rotliegend-Zechstein contact zone in the vicinity of the Żeliszowski Creek. The nearest potential source rocks of this type occur 10 km south, up the Bóbr River. In this case, the most likely direct source area of these gold grains is represented by local Oligocene quartz gravels (Fig. 2). According to Grodzicki (1969), these are the richest gold-bearing deposits of the Lwówek Śląski-Bolesławiec area, formed by redeposition of eroded adjacent Permian, Triassic and Cretaceous strata. Therefore, the source area of the gold grains does not have to be limited to the the present Permian outcrops (Speczik and Wolkowicz, 1995). Part of the gold-bearing source rocks that formed originally within the North Sudetic Basin was apparently elevated during the Laramian phase. In elevated parts of the Epi-Variscan orogen, gold-bearing clastic rocks underwent erosion and provided detritus to form younger, unlithified alluvial deposits. According to Oszczepalski et al. (2011), the Au-bearing Permian sedimentary rocks were originally deposited in the area of the present-day Fore-Sudetic Block.

Probably, the source areas of the Au-bearing alluvial sediments of the Żeliszowski Creek were not confined to the Cu-polymetallic Permian deposits of the North Sudetic Basin. Local Oligocene quartz gravels may also have been sourced

from weathered Au-bearing hydrothermal veins of the KMC (Urbański, 2010); this seems probable in view of the composition of the microinclusions and their host gold grains described in this paper. The occurrence of bismuth minerals in association with gold is similar to the mineralization of the polymetallic veins that occur around Radzimowice and Klecza-Radomice (Mikulski, 2005, 2007a, 2014).

The Na-K feldspar, quartz and Hf-bearing zircon composition of the aggregate found within the Z-3 gold grain (Fig. 19) suggests yet another origin for this particle. Hafnium is a common impurity of zircons because of the similar ionic radii of Hf and Zr atoms (Shannon, 1976; Bau, 1996). Consequently, these elements show close geochemical affinity and can replace each other within a mineral due to isovalent diadochy (Polański and Smulikowski, 1969; Polański, 1988). Therefore, both the presence of the hafnium within this zircon and its concentration are of significance here.

Hafnium occurs in nature ~40 times less frequently than zirconium (Polański, 1988), and its concentration in zircons rarely exceeds 3 wt.% (Table 1). In general, the outer, late-crystallized parts of zircons are richer in Hf than the inner parts (Wang et al., 2010). Hafnium shows a greater predisposition to concentrate within acid rather than basic igneous rocks (Brooks, 1970; Condie and Lo, 1971; Cerny et al., 1985). The highest Hf contents are found within post-magmatic rocks, especially in pegmatites (Polański and Smulikowski, 1969; Polański, 1988). Values of the Zr/Hf ratio of zircons from igneous rocks amount to 40 (Polański, 1988). According to Wang et al. (2010), this ratio varies between 4.9 and 104.5 with a mean of 39.4. By comparison, the Zr/Hf value is ~25 for pegmatite zircons (Polański, 1988), while according to Gbelsky (1979), Cerny et al. (1985) and Wang et al. (1990) it does not exceed 20 (with a Hf content of 2 to over 28 wt.%). Tables 1 and 2 show Zr/Hf ratio values and contents of Hf from zircons originating in various rock types. Compared to these, the zircon inclusion from the Z-3 gold grain is characterized by a particularly high hafnium concentration. A point analysis made in the middle of the zircon crystal indicated a content of 8.49 wt.% Hf, with a Zr/Hf ratio of 6.06. The outer rims of the zircon are enriched in hafnium,

Table 1

Hafnium contents in zircons from the various rock types

Author	Origin of the zircons examined	Hf [wt. %]
Author's own analyses	Alluvial deposits of Skora (Pielgrzymka)	2.37–3.20
	Alluvial deposits of Szreniawa (Kopacz near Złotoryja)	2.89–2.99
	Alluvial deposits of Wierzbiak (Strachowice)	2.37–3.70
	Alluvial deposits of Jamna (Łupki)	2.69–3.57
	Alluvial deposits of the Żeliszowski Creek (excluding the zircon grain from the Z-3 gold grain)	2.54
	Alluvial deposits of Kraszówka (Kraszowice)	1.19–2.86
	Alluvial deposits of the Chróśnicki Creek (Nielestno)	3.38–3.67
	Alluvial deposits of Olszanka (Wojcieszów)	0.92
	Zircon from the Z-3 gold grain (Żeliszowski Creek)	8.49
Belousova et al. (2002)	Kimberlites (Russia, South Africa, Australia)	0.57–2.3
	Lamproites (Australia, Ukraine)	0.79–1.3
	Carbonatites (Australia, Russia)	0.79–1.27
	Basalts (Australia, Thailand, Cambodia)	0.53–0.83
	Dolerites (Ukraine)	0.87–1.03
	Granitoids (Australia, Ukraine)	0.65–3.07
	Syenites (Canada, Norway)	0.59
	Larvikites	0.86–1.31
	Syenitic pegmatites (Norway)	0.68–1.92
Nephelinitic – syenitic pegmatites (Norway)	1.16–2.79	
Morawiecki (1962)	Ti-, Zr-bearing sands (Guinea)	> 2.5

Table 2

Zr/Hf ratios in zircons from various rock types

Author	Origin of the zircons examined	Zr/Hf
Author's own analyses	Alluvial deposits of Skora (Pielgrzymka)	17.04–24.27
	Alluvial deposits of Szreniawa (Kopacz near Złotoryja)	19.46–20.24
	Alluvial deposits of Wierzbiak (Strachowice)	14.95–24.88
	Alluvial deposits of Jamna (Łupki)	15.58–21.69
	Alluvial deposits of Żeliszowski Creek (excluding the zircon grain from the Z-3 gold grain)	23.04
	Alluvial deposits of Kraszówka (Kraszowice)	19.08–24.51
	Alluvial deposits of the Chróśnicki Creek (Nielestno)	15.08–16.31
	Alluvial deposits of Olszanka (Wojcieszów)	24.1
	Zircon from the Z-3 gold grain (Żeliszowski Creek)	6.06
Burda (2005)	Migmatites of Smreczyński Wierch (Tatra Mts.)	33.9–57.15
Murtezi and Kryza (2001)	Crystalline schists of Czarnów (Rudawy Janowickie)	24.0–44.0

therefore, it seems reasonable to infer a higher total concentration of Hf within the whole grain. Such hafnium-rich zircons crystallize from acid, postmagmatic solutions, probably as mineral components of granitoid pegmatites, less likely of syenitic ones.

Well-known gold-bearing pegmatites near to the sampling site occur within the Karkonosze Granite Massif. Mikulski (2007b) found, in the pegmatite of the Michałowice quarry, crystals of native gold associated with haematite, galena, sphalerite and U-Th minerals. Kozłowski (2011a) identified, in the several Karkonosze pegmatites, scarce Au mineralization represented by several crystals of native gold, the largest being 2 mm in diameter; he suggested also that veins richer in gold could originally have occurred within the currently eroded parts of the Massif.

A Scandinavian origin for the “pegmatite-type” Z-3 gold grain should also be considered. There are ~100 documented Au-polymetallic ore deposits located on the Fennoscandian Shield, represented by various genetic types (Sundblad, 2003). Kozłowski (2011b) described quartz pebbles with gold mineralization from the Western Pomerania coast. He suggested that the Au-bearing sediments could have been transported by a Scandinavian continental glacier from the territory of present-day Scandinavia and deposited south of the Baltic Sea. The Kaczawa Mountains and its Foothills were reached by the South and Middle Polish glaciations (Lindner, 1988; Marks, 2005; Marks et al., 2016). According to Muszer and Ćwiertnia (2018), the grains of native gold from the Mała Panew (right tributary of the Odra River near Opole) alluvium may be of Scandinavian origin. These grains are characterized by diameters of up to ~200 µm, distinct roundness, high purity and an Ag content of up to 2.45 wt.%. These features make these gold grains similar to the „pegmatite-type” Z-3 grain from Żeliszowski Creek.

Part of the detrital gold occurring within the Kaczawa region sediments might therefore have been glacially transported and deposited in local moraines. Such long-distance transport, although possible, was probably of minor significance for the formation of the local gold-bearing sediments. The significance of glacial and fluvio-glacial processes for development of these deposits was mainly limited to redistribution of the gold grains and formation of the secondary, gold-depleted Pleistocene and Holocene deposits.

CONCLUSIONS

1. The coexistence of primary, modified and reshaped grains within the same gold-bearing sediment directly indicates reworking of local secondary gold deposits, and the quantitative relations between the grains representing each of these groups depends on the reworking rate. This may also suggest that the gold-bearing sediments examined are polygenetic.

2. The Holocene alluvial deposits of the Lwówek Śląski-Bolesławiec area were formed by redeposition of older Cenozoic strata, combined with the contemporaneous transport and deposition of gold-bearing sediments from presently eroded source rocks. As in the previously published model for the Jamna Creek gold deposits (Kania, 2018), the alluvial gold-bearing deposits of Żeliszowski Creek seem to be polygenetic.

3. The source rocks (primary deposits) of the detrital gold investigated from the Żeliszowski Creek are represented both by local Permian red beds and quartz veins of the Kaczawa Metamorphic Complex, together with pegmatite-type deposits of unspecified location. Further analyses of the “pegmatite-type” gold grains should determine whether the source rocks of such gold grains are local (Izera-Karkonosze Block?) or not (Scandinavian?).

4. The application of the mineralogical analyses of the microinclusions within the gold grains combined with chemical and morphological investigations of the detrital gold is a useful tool for research into gold grain origin. Grains containing microinclusions are represented by various sizes, shapes and chemical composition, from electrum to pure native gold. For this reason the implemented methodology can distinguish between the grains of different origins, regardless of their morphological and chemical features.

5. This analytical method may be included in mineralogical prospecting of Au-polymetallic deposits such as those performed by Kelley et al. (2003) and Leake et al. (1995), where analyses limited to comparative chemical analyses or of grain size and morphology may be insufficient. For instance the relationship between grain size and the transport distance from a source area (Kelley et al., 2003) can be applied only to grains originating from the same, particular source. It is difficult to apply to polygenetic gold-bearing sediments, as in the Jamna (Kania, 2018) and Żeliszowski Creeks.

Comparative analyses of gold grain chemical composition should be treated with care for the same reason. This concerns both decreases in silver within Au-Ag alloys (Grodzicki, 1963, 1966, 1969; Polański, 1988) and the formation of Ag-depleted rims on grain edges (Desborough, 1970; Banaś et al., 1985; Kelley et al., 2003) with increase in transport distance of the detrital gold. In addition, the growth of depleted rims does not exclusively take place in a hypogene environment. The best evidence of this is that the rims are also present on irregu-

larly shaped, primary grains (Kania, 2018). In such cases, forming of the Ag-depleted parts of the grains may have occurred by hydrothermal leaching of chloride solutions (Kołodziej et al., 2000).

Acknowledgements. The author would like to thank the reviewers for constructive comments which helped to improve the presented manuscript. A. Muszer is thanked for expert advice, especially as regards mineralogical analyses.

REFERENCES

- Badura, J., 2013. Szczegółowa Mapa Geologiczna Polski, 1:50 000, arkusz 721 – Bolesławiec (in Polish). Państwowy Instytut Geologiczny – Państwowy Instytut Badawczy, Warszawa.
- Banaś, J., Grodzicki, A., Salamon, W., 1985. Mineralogic-geochemical characterization of detrital native gold from the vicinity of Złotoryja and Wądroże Wielkie, Lower Silesia, SW Poland. *Mineralogia Polonica*, **16**: 91–114.
- Baranowski, Z., Haydukiewicz, A., Kryza, R., Lorenc, S., Muszyński, A., Solecki, A., Urbanek, Z., 1990. Outline of the geology of the Góry Kaczawskie (Sudetes, Poland). *Neues Jahrbuch für Geologie und Paläontologie, Abhandlungen*, **179**: 223–257.
- Bau, M., 1996. Controls on the fractionation of isovalent trace elements in magmatic and aqueous systems; evidence from Y/Ho, Zr/Hf, and lanthanide tetrad effect. *Contributions to Mineralogy and Petrology*, **123**: 323–333; <https://doi.org/10.1007/s004100050159>
- Belousova, E.A., Griffin, W.L., O'Reilly, S.Y., Fisher, N.I., 2002. Igneous zircon: trace element composition as an indicator of source rock type. *Contributions to Mineralogy and Petrology*, **143**: 602–622; <https://doi.org/10.1007/s00410-002-0364-7>
- Birkenmajer, K., Jeleńska, M., Kądziołko-Hofmokr, M., Kruczyk, J., 1977. Age of deep seated fracture zones in Lower Silesia (Poland) based on K-Ar and palaeomagnetic dating on Tertiary basalts. *Annales de la Société Géologique de Pologne*, **47**: 545–552.
- Brooks C.K., 1970. The concentrations of zirconium and hafnium in some igneous and metamorphic rocks and minerals. *Geochimica et Cosmochimica Acta*, **34**: 411–416; [https://doi.org/10.1016/0016-7037\(70\)90117-1](https://doi.org/10.1016/0016-7037(70)90117-1)
- Burda, J., 2005. Morphological and geochemical characteristics of zircon crystals from Smreczyński Wierch migmatite (Western Tatra Mts.) (in Polish with English summary). *Przegląd Geologiczny*, **53**: 127–133.
- Cerny, P., Meintzer, R.E., Anderson, A.J., 1985. Extreme fractionation in rare-element granitic pegmatites: selected examples of data and mechanisms. *The Canadian Mineralogist*, **23**: 381–421.
- Choiński, A., 2007. *Limnologia fizyczna Polski* (in Polish). Wyd. Naukowe UAM, Poznań.
- Condie, K.C., Lo, H.H., 1971. Trace element geochemistry of the Louis Lake batholith of early Precambrian age, Wyoming. *Geochimica et Cosmochimica Acta*, **35**: 1099–1121; [https://doi.org/10.1016/0016-7037\(71\)90028-7](https://doi.org/10.1016/0016-7037(71)90028-7)
- Cretu, Ch., Lingen van der, E., 1999. Coloured gold alloys. *Gold Bulletin*, **32**: 115–126; <https://doi.org/10.1007/BF03214796>
- Cymerman, Z., Ilnatowicz, A., Kozdrój, W., Przybylski, B., 2009. Szczegółowa Mapa Geologiczna Polski, 1:50 000, arkusz 757 – Lubań (in Polish). Państwowy Instytut Geologiczny – Państwowy Instytut Badawczy, Warszawa.
- Cymerman, Z., Ilnatowicz, A., Kozdrój, W., Przybylski, B., 2012. Szczegółowa Mapa Geologiczna Polski, 1:50 000, arkusz 758 – Lwówek Śląski (in Polish). Państwowy Instytut Geologiczny – Państwowy Instytut Badawczy, Warszawa.
- Desborough, G.A., 1970. Silver depletion indicated by microanalysis of gold from placer occurrences, Western United States. *Economic Geology*, **65**: 304–311; <https://doi.org/10.2113/gsecongeo.65.3.304>
- DiLabio, R.N.W., 1991. Classification and interpretation of the shapes and surface textures of gold grains from till. *Gisements alluviaux d'or, La Paz*, 1–5.06: 297–313.
- Domaszewska, T., 1964. Occurrence and exploitation of gold in Lower Silesia (in Polish with English summary). *Przegląd Geologiczny*, **12**: 180–184.
- Furnes, H., Kryza, R., Muszyński, A., Pin, C., Garmann, L.B., 1994. Geochemical evidence for progressive rift-related volcanism in the eastern Variscides. *Journal of the Geological Society*, **151**: 91–109.
- Gbelsky, J., 1979. Electron microprobe determination of Zr/Hf ratios in zircons from pegmatites of the Male Karpaty Mts (West Carpathians). *Geologia Carpathica*, **30**: 463–474.
- GeoLOG. Application of the Central Geological Database (CBDG) of Polish Geological Institute – National Research Institute <<https://geolog.pgi.gov.pl>>
- Górecka, T., 1970. Results of microfloristic research of Permo-Carboniferous deposits found in the area between Jawor and Lubań (in Polish with English summary). *Geological Quarterly*, **14** (1): 52–88.
- Grodzicki, A., 1956. Szczegółowa Mapa Geologiczna Sudetów 1:25 000, arkusz Kraszowice (in Polish). Wyd. Geol., Warszawa.
- Grodzicki, A., 1963. Gold-bearing sands in the environs of Złotoryja (in Polish with English summary). *Archiwum Mineralogiczne*, **24**: 239–295.
- Grodzicki, A., 1964a. Wyjaśnienie źródła i genezy okrucowych złóż złota w okolicach Legnickiego Pola-Mikołajowic-Wądroża Wielkiego (in Polish). *Wszechświat*, **1**: 21–22. Wydawnictwo PWN.
- Grodzicki, A., 1964b. Piaski złotonosne okolic Lwówka (in Polish). *Wszechświat*, **12**: 263–265. Wydawnictwo PWN.
- Grodzicki, A., 1966. Auriferous sands from Legnickie Pole - Mikołajowice - Wądroże Wielkie (in Polish with English summary). *Archiwum Mineralogiczne*, **26**: 1–2.
- Grodzicki, A., 1969. The genesis and composition of the gold-bearing sands of Lwówek Śląski and Bolesławiec area (in Polish with English summary). *Acta Universitatis Wratislaviensis, Prace Geologiczno-Mineralogiczne*, **86**: 99–129.
- Grodzicki, A., 1972. On the petrography and mineralogy of the gold-bearing sands of Lower Silesia (in Polish with English summary). *Geologia Sudetica*, **6**: 233–291.
- Grodzicki, A., 1989. Metoda denudodezagregacji i jej zastosowanie w badaniach skał okrucowych (in Polish with English summary). *Acta Universitatis Wratislaviensis, Prace Geol. Mineral.*, **16**: 5–270.
- Grodzicki, A., 1990. The genesis and finding possibilities of some heavy minerals in Lower Silesia (in Polish with English summary). *Physicochemical Problems of Mineral Processing*, **23**: 19–25.

- Grodzicki, A., 1997.** Piaski złotońosne Dolnego Śląska w świetle teorii denudodezagregacji (in Polish). In: *Metale szlachetne w NE części Masywu Czeskiego i w obszarach przyległych: geneza, występowanie, perspektywy* (ed. A. Muszer): 95–98. Conference materials, Jarnołtówek, 19–21.06.1997.
- Grodzicki, A., 1998.** Litostratigraphy, petrography and mineralogy of Cainozoic gold-bearing sands from Lower Silesia (in Polish with English summary). *Physicochemical Problems of Mineral Processing*, **32**: 31–41.
- Grodzicki, A., 2011.** Placer gold in Sudetes Mountains and in their foreland. *Archivum Mineralogiae Monograph*, **2**: 191–208.
- Hérail, G., Fornar, G., Viskarra, G., Miranda, V., 1990.** Morphological and chemical evolution of gold grains during formation of a polygenetic fluvialite placer: the Mio-Pleistocene Tipuani placer example (Andes, Bolivia). *Chronicle of mineral research and exploration*, **500**: 41–49.
- Jęczmyk, M., Krzemińska, E., 1996.** Skład chemiczny złota okruszowego w utworach aluwialnych Pogórza Izerskiego (in Polish). *Przegląd Geologiczny*, **44**: 285–290.
- Kanasiewicz, J., 1964.** Some remarks on the occurrence of native selenium (in Polish with English summary). *Przegląd Geologiczny*, **12**: 390–391.
- Kanasiewicz, J., 1966.** Geochemical profile of uranium, selenium and rhenium in the Zechstein of the Leszczyna Trough (in Polish with English summary). *Geological Quarterly*, **10** (2): 309–314.
- Kanasiewicz, J., 1967.** Occurrence of rare elements in the copper-bearing marl series of the Lower Zechstein in the Grodziec Syncline (in Polish with English summary). *Geological Quarterly*, **11** (1): 113–117.
- Kania, M., 2018.** Application of the chemical-mineralogical assays of placer gold grains in the prospection of the polymetallic mineralisation (in Polish with English summary). *Górnictwo Odkrywkowe*, **3**: 115–122.
- Kania, M., 2020.** Detrital gold origin research methodology (in Polish with English summary). *Górnictwo Odkrywkowe*, **4**: 25–34.
- Kania, M., Muszer, A., 2017.** Characteristics of Hg-bearing gold from selected areas of Lower Silesia (in Polish with English summary). *Górnictwo Odkrywkowe*, **5**: 11–21.
- Karnkowski, P.H., 1999.** Origin and evolution of the Polish Rotliegend Basin. *Polish Geological Institute, Special Papers*, **3**: 1–93.
- Kelley, D.L., Brommecker, R., Averill, S.A., 2003.** Forecasting lode gold potential from physical and chemical characteristics of placer gold grains - an example from French Guiana. In: *International Geochemical Exploration Symposium. North Atlantic Minerals Symposium 2003, Programme and Abstracts*: 42–43; https://www.appliedgeochemists.org/images/stories/IEGS_2003/O36_Kelley_IGESnotes.pdf
- Kiersnowski, H., Paul, J., Peryt, T.M., Smith, D., 1995.** Facies, palaeogeography and sedimentary history of the Southern Permian Basin in Europe. In: *The Permian of Northern Pangea* (ed. P. Scholle, T.M. Peryt, D.S. Ulmer-Scholle), **2**: 119–136. Springer-Verlag, Berlin; https://doi.org/10.1007/978-3-642-78590-0_7
- Kołodziej, B., Muszer, A., Adamski, Z., 2000.** Investigation of Au-Ag alloy behaviour in chloride solutions (in Polish with English summary). *Physicochemical Problems of Mineral Processing, XXXVII Symposium*, **25**: 15–23.
- Konstantynowicz, E., 1965.** Mineralizacja utworów cechsztynu niecki północnosudeckiej (in Polish). *Prace Geologiczne*, **18**: 7–99.
- Konstantynowicz, E., 1971.** Monografia przemysłu miedziowego w Polsce (in Polish). T. 1. Wyd. Geol., Warszawa.
- Kozłowski, A., 2011a.** Native gold in the intragranitic pegmatites of the Karkonosze massif. *Archivum Mineralogiae Monograph*, **2**: 9–25.
- Kozłowski, A., 2011b.** Native gold in quartz pebbles of the Baltic shore, West Pomerania. *Archivum Mineralogiae Monograph*, **2**: 353–367.
- Kozłowski, S., Parachoniak, W., 1967.** Wulkanizm permski w depresji północnosudeckiej (in Polish). *Prace Muzeum Ziemi*, **11**: 192–222.
- Kryza, R., 2008.** The Variscan Kaczawa Complex: witness of Palaeozoic basins and Variscan orogeny. In: *Geoeducational potential of the Sudety Mts.* (ed. A. Solecki): 17–26. University of Wrocław, Institute of Geological Sciences.
- Kucha, H., Przybyłowicz, W., 1999.** Noble metals in organic matter and clay-organic matrices, Kupferschiefer, Poland. *Economic Geology*, **94**: 1137–1162; <https://doi.org/10.2113/gsecongeo.94.7.1137>
- Kucha, H., Mayer, W., Piestrzyński, A., 1982.** Mineralogy and geochemistry of silver in the Konrad mine (in Polish with English summary). *Rudy i Metale Nieżelazne*, **27**: 254–258.
- Leake, R.C., Styles, M.T., Bland, D.J., Henney, P.J., Wetton, P.D., Naden, J., 1995.** The interpretation of alluvial gold characteristics as an exploration technique. *British Geological Survey, ODA Technical Report WC/95/22, Overseas Geology Series*. Keyworth, Nottingham.
- Lindner, L., 1988.** Stratigraphy and extents of Pleistocene continental glaciations in Europe. *Acta Geologica Polonica*, **38**: 63–83.
- Loen, J.S., 1995.** Use of placer gold characteristics to locate bedrock gold mineralization. *Exploration and Mining Geology*, **4**: 335–339.
- Łuszczkiewicz, A., Muszer, A., 1999.** Gold from Rakowice placer deposit near Lwówek Śląski, SW Poland (in Polish with English abstract). *Physicochemical Problems of Mineral Processing*, **33**: 99–106.
- Marks, L., 2005.** Pleistocene glacial limits in the territory of Poland. *Przegląd Geologiczny*, **53**: 988–993.
- Marks, L., Dzierżek, J., Janiszewski, R., Koczorowski, J., Lindner, L., Majecka, A., Makos, M., Szymanek, M., Toloczko-Pasek, A., Woronko, B., 2016.** Quarternary stratigraphy and palaeogeography of Poland. *Acta Geologica Polonica*, **66**: 403–427; <https://doi.org/10.1515/agp-2016-0018>
- Mastalerz, K., Raczyński, P., 1993.** Litostratigrafia i ewolucja basenu północnosudeckiego w karbonie i permie (in Polish). In: *Baseny sedimentacyjne: procesy, osady, architektura* (ed. K. Mastalerz, L. Kurowski and P. Raczyński): 90–97. *Przewodnik II Krajowego Spotkania Sedymetologów*. Instytut Nauk Geologicznych Uniwersytetu Wrocławskiego.
- Mikułski, S.Z., 2005.** Geological, mineralogical and geochemical characteristics of the Radzimowice Au-As-Cu deposit from the Kaczawa Mts. (Western Sudetes, Poland) – an example of the transition of porphyry and epithermal style. *Mineralium Deposita* **39**: 904–920; <https://doi.org/10.1007/s00126-004-0452-x>
- Mikułski, S.Z., 2007a.** The late Variscan gold mineralization in the Kaczawa Mountains, Western Sudetes. *Polish Geological Institute Special Papers*, **22**: 1–162.
- Mikułski, S.Z., 2007b.** Metal ore potential of the parent magma of granite – the Karkonosze massif example. *Archivum Mineralogiae Monograph*, **1**: 123–145.
- Mikułski, S.Z., 2007c.** Powstanie pierwotnych złóż złota w Górach Kaczawskich a procesy geotektoniczne w karbonie i permie (in Polish). *Przegląd Geologiczny*, **55**: 299–300.
- Mikułski, S.Z., 2014.** The occurrence of tellurium and bismuth in the gold-bearing polymetallic sulfide ores in the Sudetes (SW Poland) (in Polish with English summary). *Gospodarka Surowcami Mineralnymi*, **30**: 15–34; <https://doi.org/10.2478/gospo-2014-0019>
- Mikułski, S.Z., Wierchowicz, J., 2013.** Placer scheelite and gold from alluvial sediments as indicators of primary mineralisation – examples from SW Poland. *Geological Quarterly*, **57** (3): 503–514; <https://doi.org/10.7306/gq.1107>
- Mikułski, S.Z., Williams, I.S., 2014.** Zircon U-Pb dating of igneous rocks in the Radzimowice and Wielisław Złotyryjski auriferous polymetallic deposits, Sudetes, SW Poland. *Annales Societatis Geologorum Poloniae*, **84**: 213–233.
- Milewicz, J., 1959.** Szczegółowa mapa geologiczna Sudetów 1:25 000, arkusz Lwówek Śląski (in Polish). Instytut Geologiczny, Warszawa.
- Milewicz, J., 1997.** Upper Cretaceous of the North Sudetic depression. Litho- and biostratigraphy, tectonics and remarks on raw materials (in Polish with English summary). *Acta Universitatis Wratislaviensis, Prace Geologiczno-Mineralogiczne*, **61**: 1–58.

- Mizerski, W., Żukowski, J. (ed.), 2001.** Tablice geograficzne (in Polish). Wyd. Adamantan, Warszawa. Wyd. VIII.
- Morawiecki, A., 1962.** Titanium-zircon sands from Cape Verga in Guinea (in Polish with English summary). *Kwartalnik Geologiczny*, **6** (4): 229–245.
- Murtezi, M., Kryza, R., 2001.** Zircon as petrogenetic indicator in the Czarnów schists. East Karkonosze Complex, SW Poland (in Polish with English summary). *Przegląd Geologiczny*, **49**: 815–819.
- Muszer, A., 2011.** Analysis of the technological possibilities of the recovery of gold and other metals during the underwater exploitation of gravel in the Lwówek region (in Polish with English summary). *Górnictwo Odkrywkowe*, **6**: 141–146.
- Muszer, A., Ćwiertnia, J., 2018.** Characteristics of the native gold from Mała Panew River in Luboszyce near Opole (in Polish with English summary). *Górnictwo Odkrywkowe*, **3**: 111–114.
- Muszer, A., Ćwiertnia, J., Kania, M., 2016.** Anthropogenic gold from Złotyja area (Kaczawa Foothills) (in Polish with English summary). *Górnictwo Odkrywkowe*, **4**: 5–11.
- Oszczepalski, S., 1989.** Kupferschiefer in southwestern Poland: sedimentary environments, metal zoning, and ore controls. *Geological Association of Canada Special Paper*, **36**: 571–600.
- Oszczepalski, S., 1999.** Origin of the Kupferschiefer polymetallic mineralization in Poland. *Mineralium Deposita*, **34**: 599–613; <https://doi.org/10.1007/s001260050222>
- Oszczepalski, S., 2007.** Au-Pt-Pd mineralization in the Zechstein Kupferschiefer series on the reserved areas for copper mining (in Polish with English summary). *Biuletyn Państwowego Instytutu Geologicznego*, **423**: 109–124.
- Oszczepalski, S., Rydzewski, A., 1995.** Zechstein polymetallic mineralization on the Żary pericline. *Prace Państwowego Instytutu Geologicznego*, **151**: 23–34.
- Oszczepalski, S., Rydzewski, A., 1997.** Atlas metalogeniczny cechsztyńskiej serii miedzionośnej w Polsce (in Polish). *PIG*, Wyd. Kartograficzne Polskiej Agencji Ekologicznej S.A., Warszawa.
- Oszczepalski, S., Speczik, S., Wojciechowski, A., 2011.** Gold mineralization in the Kupferschiefer oxidized series of the North Sudetic trough, SW Poland. *Archivum Mineralogiae Monograph*, **2**: 153–168.
- Pieczonka, J., Piestrzyński, A., 2011.** Gold and other precious metals in copper deposit, Lubin-Sieroszowice district, SW Poland. *Archivum Mineralogiae Monograph*, **2**: 135–152.
- Pieczonka, J., Piestrzyński, A., Mucha, J., Głuszek, A., Kotarba, M., Więclaw, D., 2008.** The red-bed-type precious metal deposit in the Sieroszowice-Polkowice copper mining district, SW Poland. *Annales Societatis Geologorum Poloniae*, **78**: 151–280.
- Pieczonka, J., Piestrzyński, A., 2015.** Precious metals in the copper deposit of the Fore-Sudetic Monocline, SW Poland, a new data (in Polish with English summary). *CUPRUM*, **76**: 7–17.
- Piesterzyński, A., Pieczonka, J. 1998.** Tetraauricupride from the Kupferschiefer type deposit, SW Poland – the first occurrence. *Mineralogia Polonica*, **29**: 11–18.
- Piesterzyński, A., Wodzicki, A., 2000.** Origin of the gold deposit in the Polkowie-West mine, Lubin-Sieroszowice Mining District, Poland. *Mineralium Deposita*, **35**: 37–47; <https://doi.org/10.1007/s001260050004>
- Piesterzyński, A., Pieczonka, J., Speczik, S., Oszczepalski, S., Banaszak, A., 1997.** Noble metals from the Kupferschiefer-type deposits, Lubin-Sieroszowice, SW Poland. In: *Mineral Deposits* (ed. H. Papunen): 563–566. Balkema, Rotterdam.
- Piesterzyński, A., Pieczonka, J., Głuszek, A., 2002.** Redbed-type gold mineralisation, Kupferschiefer, South-West Poland. *Mineralium Deposita*, **37**: 512–528; <https://doi.org/10.1007/s00126-002-0256-9>
- Polański, A., 1988.** Podstawy geochemii (in Polish). Wyd. Geol., wyd. I, Warszawa.
- Polański, A., Smulikowski, K., 1969.** Geochemia (in Polish). Wyd. Geol., wyd. I, Warszawa.
- Przybylski, B., Ihnatowicz, A., 2013.** Szczegółowa mapa geologiczna Polski, 1:50 000, arkusz 720 – Nowogrodzic (in Polish). Państwowy Instytut Geologiczny – Państwowy Instytut Badawczy, Warszawa.
- Quiring, H., 1913.** Über das Goldvorkommen bei Goldberg in Schlesien und seine bergmännische Gewinnung im 13 und 14 Jahrhundert – Jahresbericht der schlesischen Gesellschaft für vaterländische Kultur (in German). Breslau.
- Quiring, H., 1914.** Beiträge zur Kenntnis der niederschlesischen Goldvorkommen (in German). *Zeitschrift für praktische Geologie*, **22**.
- Raczyński, P., 1997.** Depositional conditions and paleoenvironments of the Zechstein deposits in the North-Sudetic Basin (SW Poland) (in Polish with English summary). *Przegląd Geologiczny*, **45**: 693–699.
- Rentzsch, J., Langer, M., 1963.** Fazielle Probleme des Kupferschiefers von Spremberg-Weisswasser. *Zeitschrift für Angewandte Geologie*, **10**: 507–513; <https://doi.org/10.1515/9783112559024-003>
- Romaniec, E., Janiec, R., 1957.** Opracowanie geologiczne złoża miedzi rejonu „Nowy Kościół” (in Polish). *CAG-PIG-PIB*, nr arch. 4422/194.
- Saeger, K.E., Rodies, J., 1977.** The colour of gold and its alloys: The mechanism of variation in optical properties. *Gold Bulletin*, **10**: 10–14; <https://doi.org/10.1007/BF03216519>
- Schumacher, F., 1924.** Die Goldvorkommen der Gegend von Löwenberg in Niederschlesien (in German). *Zeitschrift für praktische Geologie*, **32**: 6–11.
- Shannon, R.D., 1976.** Revised effective ionic radii and systematic studies of interatomic distances in halide and chalcogenides. *Acta Crystallographica*, **A32**: 751–767; <https://doi.org/10.1107/S0567739476001551>
- Skowronek, C., 1968.** Red spots in the Lower Zechstein (in Polish with English summary). *Rudy i Metale Nieżelazne*, **13**: 134–137.
- Solecki, A., 1995.** Joints and shears of the N Sudetic Synclinorium. In: *Mechanics of Jointed and Faulted Rocks* (ed. H.P. Rossmanith): 341–346. *Proc. Of the 2nd International Conference of the mechanics of Jointed and Faulted Rock*. Balkema, Rotterdam.
- Solecki, A., 2008.** The North-Sudetic Synclinorium - geosites of the inverted basin setting. In: *Geoeducational potential of the Sudety Mts* (ed. A. Solecki A.): 17–26. University of Wrocław, Institute of Geological Sciences, Wrocław.
- Solecki, A., 2011.** Structural development of the epi-Variscan cover in the North Sudetic Synclinorium area (in Polish with English summary). In: *Mezozoik i kenozoik Dolnego Śląska* (ed. A. Żelaźniewicz, J. Wojewoda and W. Ciężkowski): 19–36. WIND, Wrocław.
- Speczik, S., Wojciechowski, A., 1997.** Gold-bearing Rotliegend-Zechstein transition sediments of the North Sudetic Trough near Nowy Kościół (SW Poland) (in Polish with English summary). *Przegląd Geologiczny*, **45**: 872–874.
- Speczik, S., Wołkowicz, W., 1995.** Origin of alluvial gold – a case study of Bóbr river deposits. In: *Mineral deposits: from their origin to their environmental impacts* (ed. J. Pasava et al.): 195–198. *Proc. 3rd Biennial SGA Meeting*. Prague, 28–31 August 1995. Balkema, Rotterdam.
- Speczik, S., Rydzewski, A., Oszczepalski, S., Piesterzyński, A., 1997.** Exploration for Cu-Ag and Au-Pt-Pd Kupferschiefer-type deposits in SW Poland. In: *Mineral Deposits* (ed. H. Papunen): 119–122. Balkema, Rotterdam.
- Speczik, S., Oszczepalski, S., Nowak, G.J., Grotek, I., Niczyporuk, K., 2003.** Organic matter alteration trends in the Polish Kupferschiefer: ore genetic implications. In: *Mineral Exploration and Sustainable Development* (ed. D.G. Eliopoulos): 853–856. Millpress, Rotterdam.
- Sundblad, K., 2003.** Metallogeny of gold in the precambrian of northern Europe. *Economic Geology*, **98**: 1271–1290; <https://doi.org/10.2113/gsecongeo.98.7.1271>
- Śliwiński, W., Raczyński, P., Wojewoda, J., 2003.** Sedymentacja utworów pokrywy osadowej w basenie północnosudeckim (in Polish). In: *Sudety zachodnie: od wendy do czwartorzędu* (ed. A. Ciężkowski, J. Wojewoda and A. Żelaźniewicz): 119–126. WIND, Wrocław.

- Townley, B.K., Hérail, G., Maksaev, V., Palacios, C., de Parseval, P., Sepulveda, F., Orellana, R., Rivas, P., Ulloa, C., 2003.** Gold grain morphology and composition as an exploration tool: application to gold exploration in covered areas. *Geochemistry: Exploration, Environment, Analysis*, 3: 29–38; <https://doi.org/10.1144/1467-787302-042>
- Urbański, P., 2010.** Gold-bearing deposits of the Kraszówka stream (Kaczawskie Foothills) (in Polish with English summary). *Biuletyn Państwowego Instytutu Geologicznego*, 439: 375–388.
- Wang, R.C., Monchoux, P., Fontan, F., 1990.** Chemical composition of the Hafnium-rich zircon from the Beauvoir granite (the Echassieres granitic complex, France) and their relationships with cassiterite. *Journal of Nanjing University (Earth Science)*, 2: 59–68.
- Wang, X., Griffin, W.L., Chen, J., 2010.** Hf contents and Zr/Hf ratios in granitic zircons. *Geochemical Journal*, 44: 65–72; <https://doi.org/10.2343/geochemj.1.0043>
- Wierchowicz, J., 2002.** Morphology and chemistry of placer gold grains - indicators of the origin of the placers: an example from the East Sudetic Foreland, Poland. *Acta Geologica Polonica*, 52: 563–576.
- Wierchowicz, J., 2010.** Gold in technogenous placers of Lower Silesia, Poland. Warsaw University Press.
- Wierchowicz, J., 2011.** Placer gold of East Sudetes and its foreland, Poland. *Archivum Mineralogiae Monograph*, 2: 209–242.
- Wierchowicz, J., Zieliński, K., 2017.** Origin of placer gold and other heavy minerals from fluvial Cenozoic sediments in close proximity to Rote Fäule-related Au mineralisation in the North Sudetic Trough, SW Poland. *Geological Quarterly*, 61 (1): 62–80; <https://doi.org/10.7306/gq.1315>
- Wierchowicz, J., Mikulski, S.Z., Gąsiński, A., 2018.** Nanoforms of gold from abandoned placer deposits of Wądroże Wielkie, Lower Silesia, Poland – the evidence of authigenic gold mineralization. *Ore Geology Reviews*, 101: 211–220; <https://doi.org/10.1016/j.oregeorev.2018.07.009>
- Wierchowicz, J., Mikulski, S.Z., Zieliński, K., 2021.** Supergene gold mineralization from exploited placer deposits at Dziwiszów in the Sudetes (NE Bohemian Massif, SW Poland). *Ore Geology Reviews*, 131, April 2021, 104049; <https://doi.org/10.1016/j.oregeorev.2021.104049>
- Wojciechowski, A., 1998.** Geochemiczne i facjalne wykształcenie złotośnych osadów ilastych cechsztynu w rejonie Złotoryja-Nowy Kościół-Leszczyna (in Polish). *CAG PIG-PIB*, 5/99.
- Wojciechowski, A., 2001.** Rotliegend/Zechstein gold-bearing horizon in the North Sudetic Trough near Nowy Kościół (SW Poland) (in Polish with English summary). *Przegląd Geologiczny*, 49: 5–62.
- Wojciechowski, A., 2011.** Gold and copper in the western part of the North-Sudetic Trough. *Archivum Mineralogiae Monograph*, 2: 169–177.
- Yushko-Zakharova, O.E., Ivanov, V.V., Soboleva, L.N. (ed.), 1986.** Minerale blagorodnych metallov (in Russian). Nedra, Moskwa.
- Żelaźniewicz, A., Aleksandrowski, P., Buła, Z., Karnkowski, P.H., Konon, A., Oszczytko, N., Ślącza, A., Żaba, J., Żytko, K., 2011.** Regionalizacja tektoniczna Polski (in Polish). *Komitet Nauk Geologicznych PAN, Wrocław*.

APPENDIX 1

For the EDS analyses, the polished sections with gold grains were graphite-coated. Each measurement session was preceded by calibration (*Energy-Channel Calibration/Energy-Axis Calibration*), in accordance with the recommendations of Bruker, the producer of the EDS detectors and analytical software. Calibrations were performed using a copper standard because of the large difference of the critical ionization values between the K, L and M lines, which provides a more precise match between analysed and theoretical spectra.

The following setting was applied: electron acceleration of 25 keV, current of 15 nA, spot size from 5 to 500 nm. Processing of the characteristic X-ray spectra was performed by *Bruker Esprit v1.9* software. Point analyses of the particular grains were preceded by surface mapping of the following elements: Ag, As, Au, Bi, Cd, Co, Cr, Cu, Fe, Hg, Ir, Mn, Mo, Ni, Os, Pb, Pd, Pt, Rh, Ru, S, Sb, Se, Si, Sn, Te, Ti, V, W, Zn. These elements are present in most common ore- and rock-forming minerals accompanying Au mineralization, and some (Ag, Cu, Hg, PGE, Te, Bi) co-create natural gold alloys, e.g. electrum (Mikulski, 2007a; Kania and Muszer, 2017; Kania, 2018), maldonite (Mikulski, 2007a), tetraauricupride (Piestrzyński and Pieczonka, 1998), Au-Ag-Pd-Hg alloys (Wierchowicz and Zieliński, 2017). The spatial distribution of these elements was used to identify the microinclusions and phases, which could be missed during examination in reflected light. The selected gold grains with a complex phase composition of Au-Ag-Hg-Cu were also examined by linear analyses. Close attention was paid to silver, the most frequently-occurring metal which coexists with gold. Both of these elements co-create phase series of unlimited miscibility. To determine the Au-Ag phase, the Yushko-Zakharova et al. (1986) classification was adopted.

Acquisition time of the EDS analyses was 60, 90 and 120 s, respectively for point, linear and mapping analyses. The extended acquisition time allowed gathering over a million counts for a single spectrum, which authenticated the results of the semi-quantitative analyses of the trace elements. The PB-ZAF procedure was adopted during quantification of the data, as well as in correction for the coating element (Carbon Correction).

The spectra acquired were interpreted manually with particular attention to fake peaks (*artefacts*), especially summary ones, which usually formed in the 4.5–5.0 keV range as an effect of the Au $M\alpha$ peak creation. The shapes of the Bremsstrahlung spectra were also fitted manually. Moreover, a *deconvolution* tool built into the software was used. This allows comparison of the theoretical, summary spectra of the chosen elements with the real ones acquired during analysis. As a result, the presence of particular elements within the measured sample can be precisely evaluated and, if required, these elements can be deleted or new elements can be added into the spectra. This procedure allowed careful evaluation of Au and Hg ($M\alpha$ line) or Ag and Pd coexistence (lines $L\alpha$ – $L\beta$). A content of 0.1 wt % was adopted as a detection limit for the particular element. The EDS characteristic spectra and elemental compositions of the microinclusions were identified within the gold grains examined from the Żeliszowski Creek channel-fill deposits:

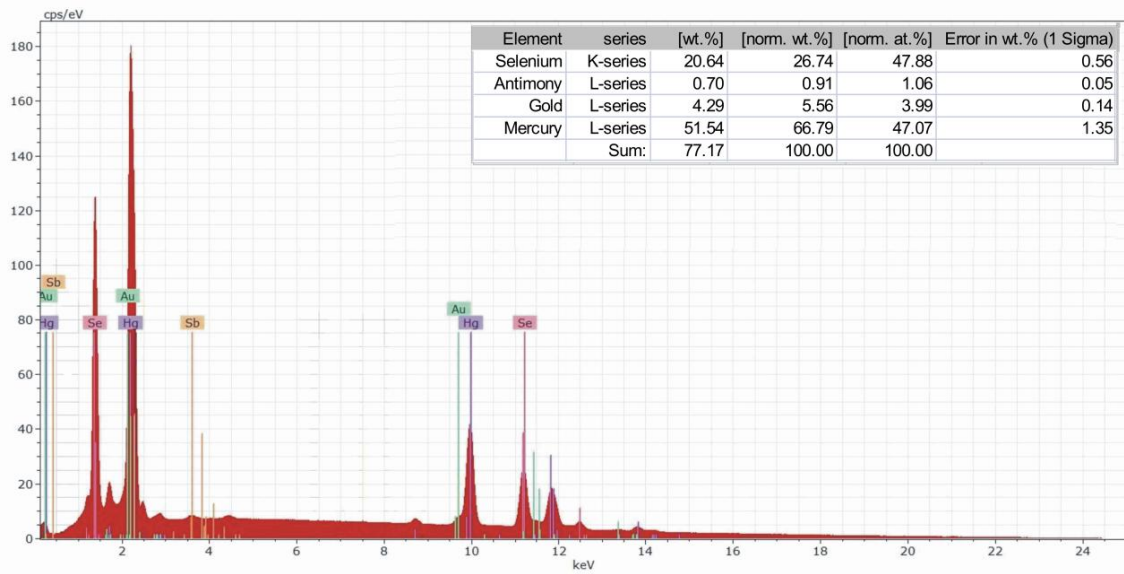


Fig. I. X-ray spectrum and results of the point analysis Z-1.I – selenide with the elemental composition of tiemannite within the Z-1 gold grain

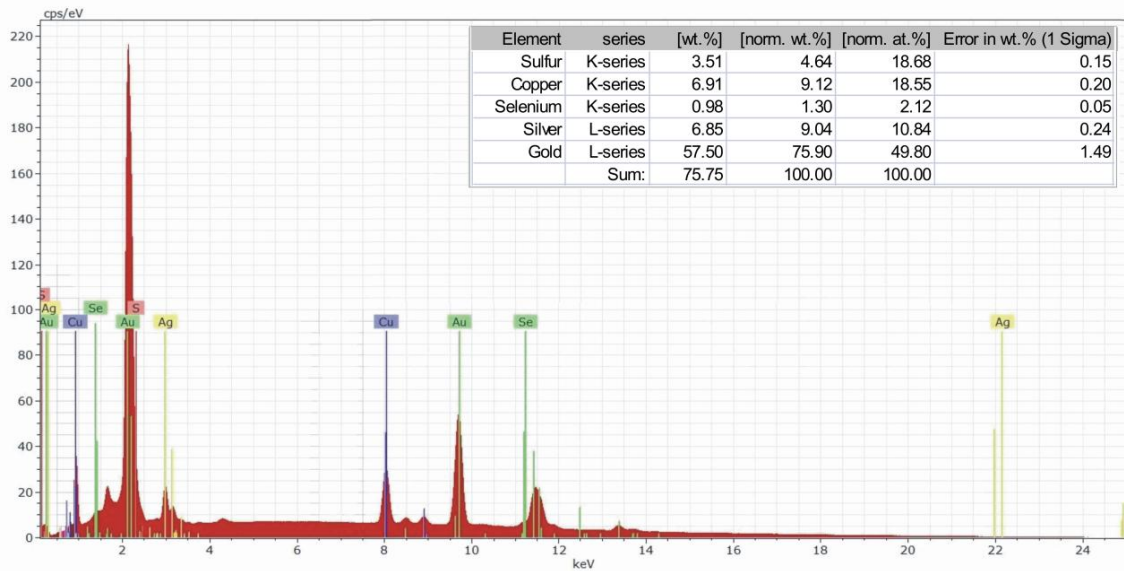


Fig. II. X-ray spectrum and results of the point analysis Z-1.II – sulphide with the elemental composition of covellite within the Z-1 gold grain

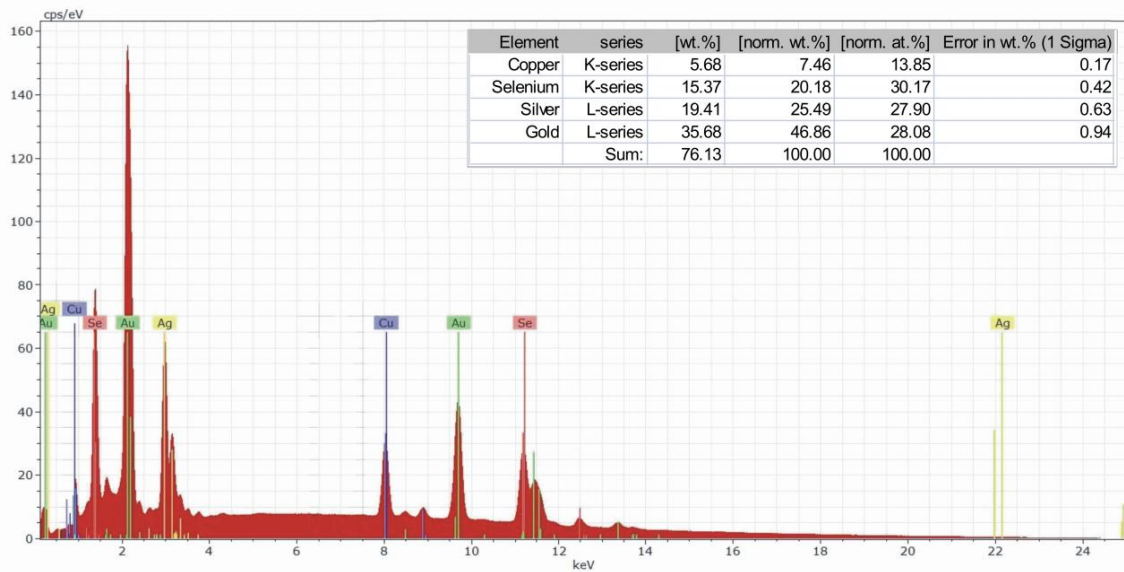


Fig. III. X-ray spectrum and results of the point analysis Z-1.II – selenide with the elemental composition of fischesserite within the Z-1 gold grain

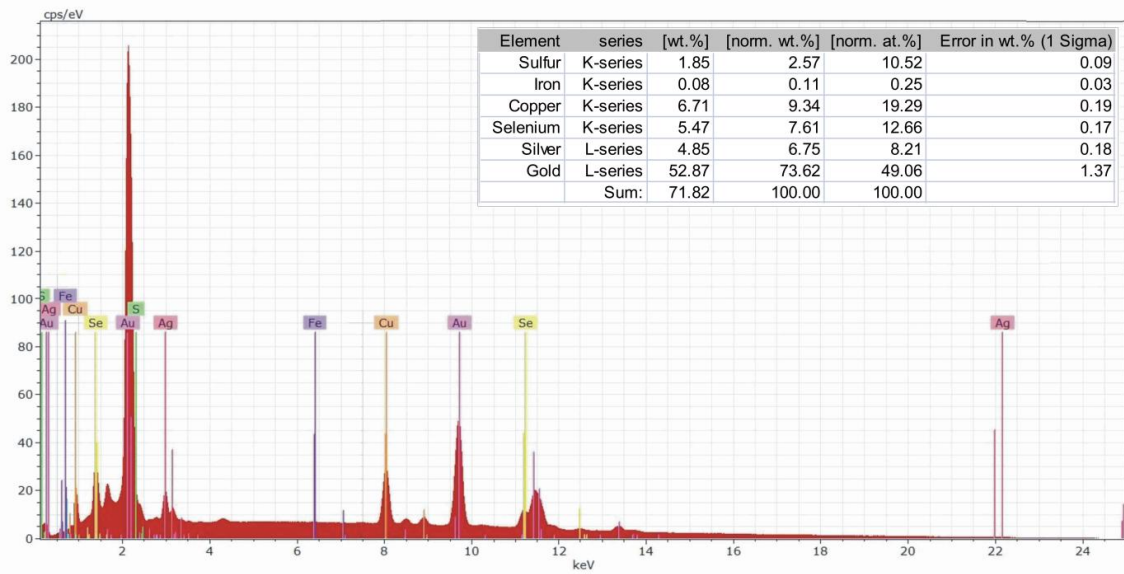


Fig. IV. X-ray spectrum and results of the point analysis Z-1.IV – biphas microinclusion with the elemental composition of Klockmannite-covellite within the Z-1 gold grain

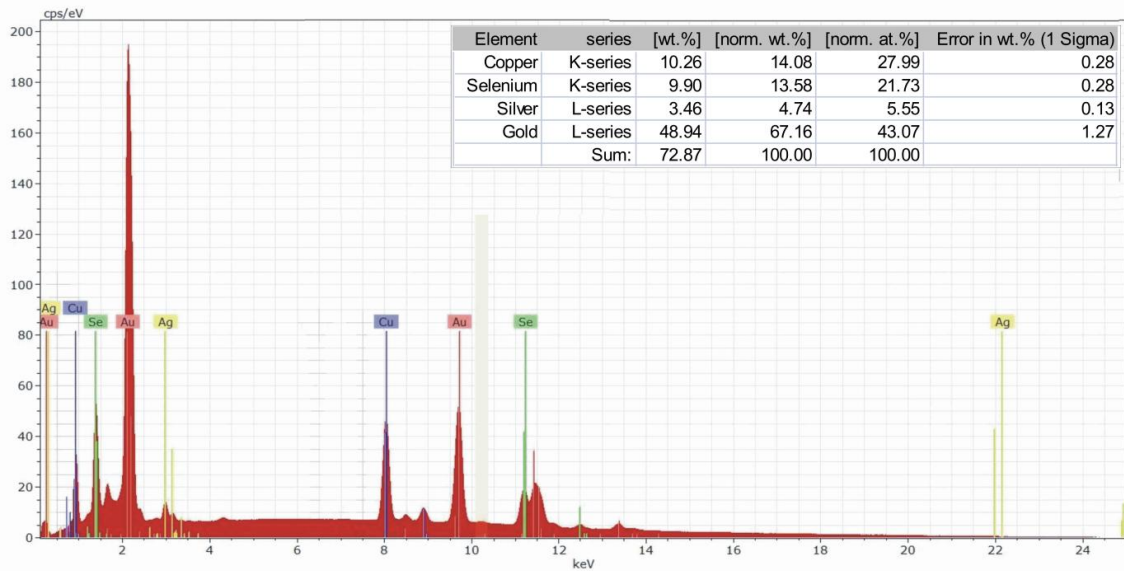


Fig. V. X-ray spectrum and results of the point analysis Z-1.V – selenide with the elemental composition of athabascaite within the Z-1 gold grain

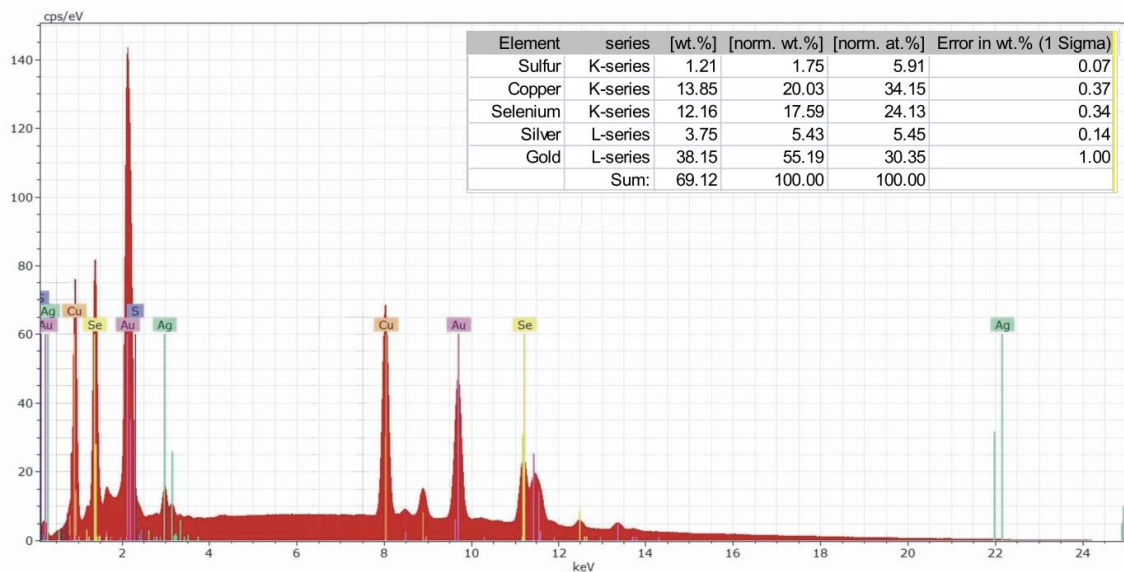


Fig. VI. X-ray spectrum and results of the point analysis Z-1.VI – selenide with the elemental composition of Klockmannite within the Z-1 gold grain

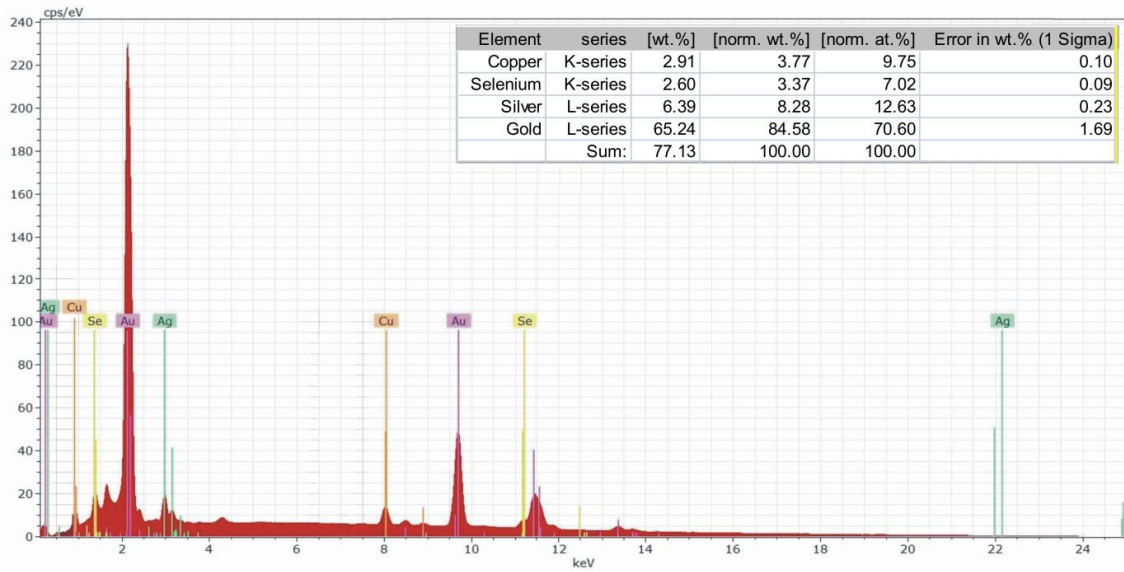


Fig. VII. X-ray spectrum and results of the point analysis Z-1.VII – microinclusion with the intermediate composition of athabascaite-umangite within the Z-1 gold grain

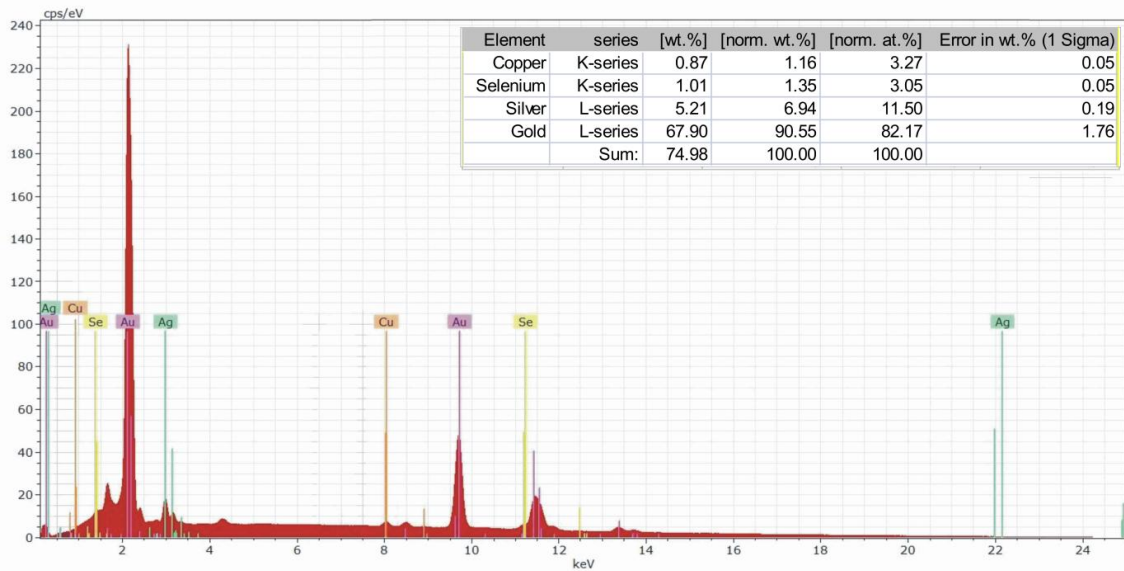


Fig. VIII. X-ray spectrum and results of the point analysis Z-1.VIII – selenide with the elemental composition of kloekmannite within the Z-1 gold grain

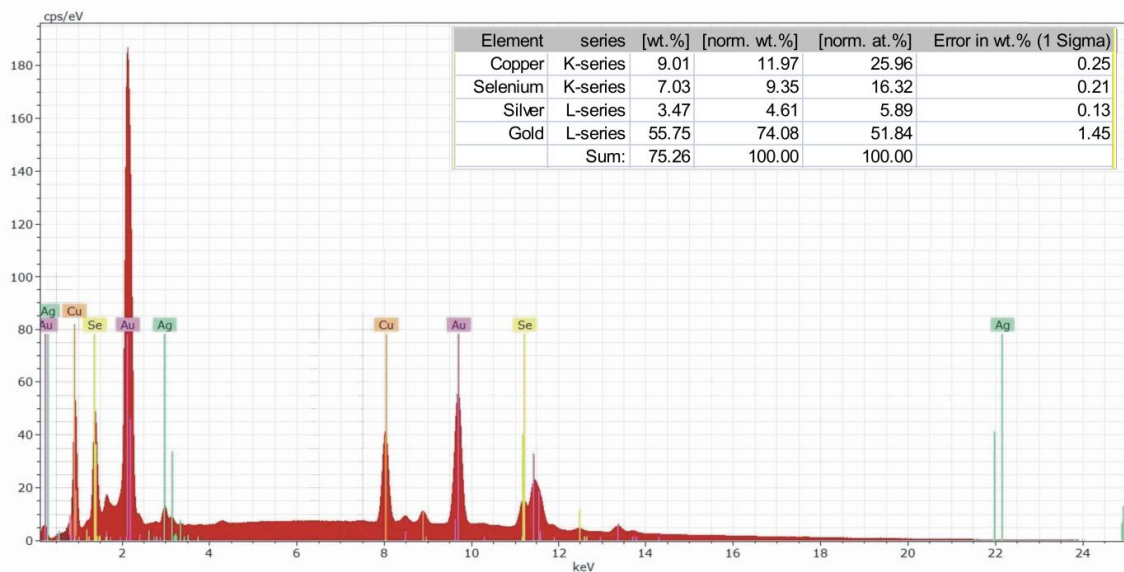


Fig. IX. X-ray spectrum and results of the point analysis Z-1.IX – selenide with the elemental composition of umangite within the Z-1 gold grain

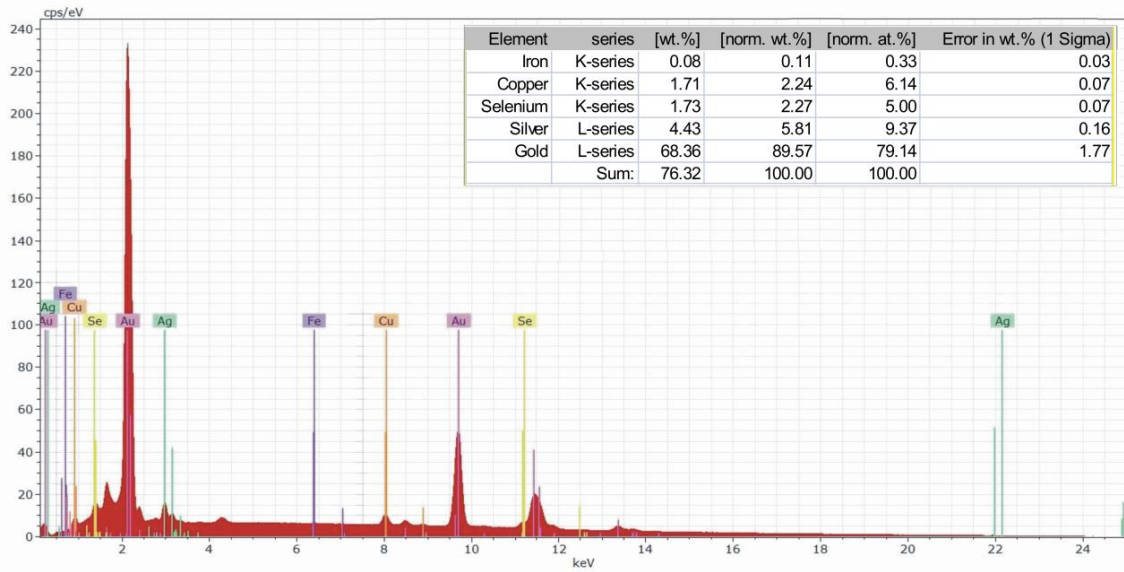


Fig. X. X-ray spectrum and results of the point analysis Z-1.X – selenide with the elemental composition of athabascaite within the Z-1 gold grain

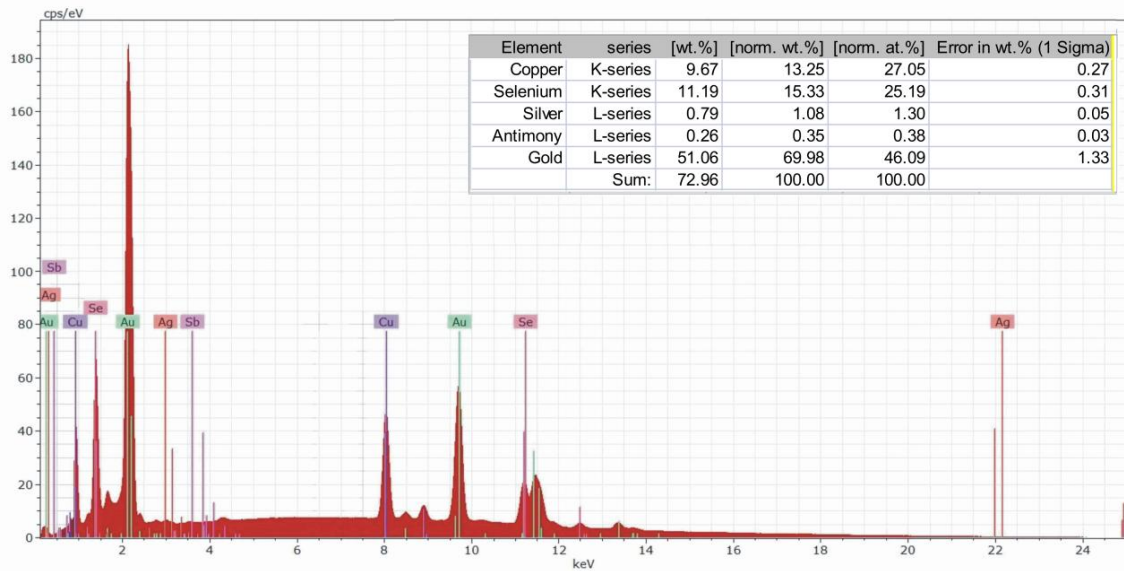


Fig. XI. X-ray spectrum and results of the point analysis Z-1.XI – selenide with the elemental composition of klockmannite within the Z-1 gold grain

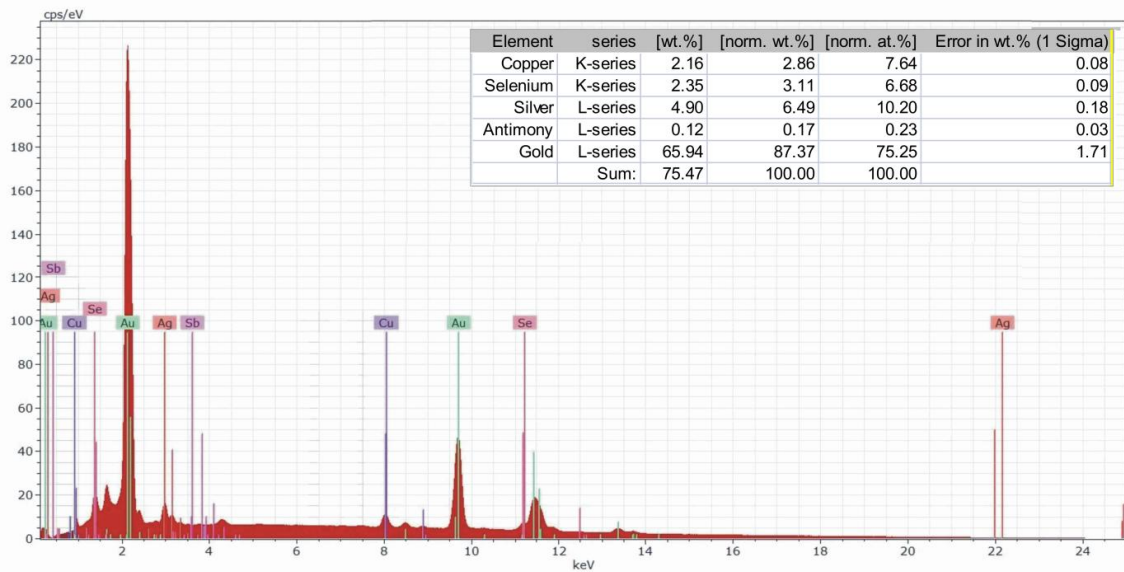


Fig. XII. X-ray spectrum and results of the point analysis Z-1.XII – selenide with the elemental composition of klockmannite within the Z-1 gold grain

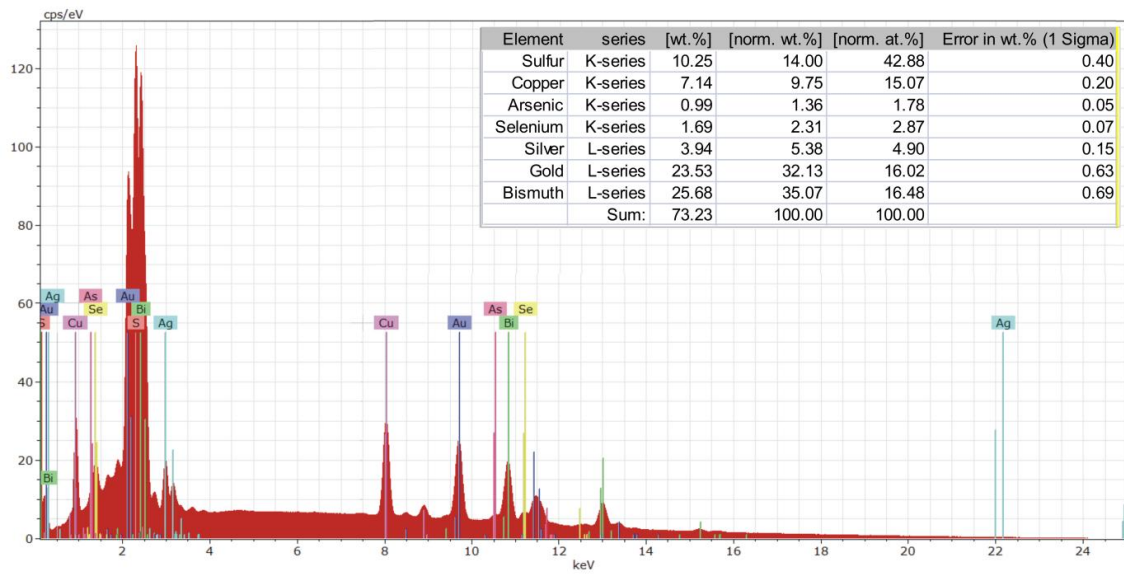


Fig. XIII. X-ray spectrum and results of the point analysis Z-11.I – biphasic microinclusion with the elemental composition of covellite - bismuthinite within the Z-11 gold grain

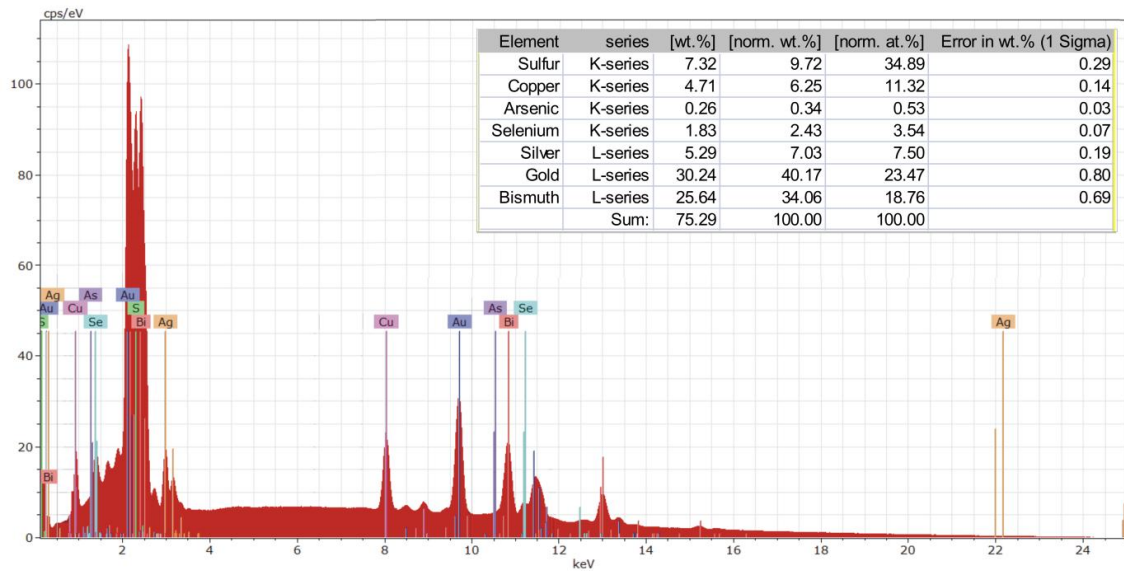


Fig. XIV. X-ray spectrum and results of the point analysis Z-11.II – biphasic microinclusion with the elemental composition of covellite-bismuthinite within the Z-11 gold grain

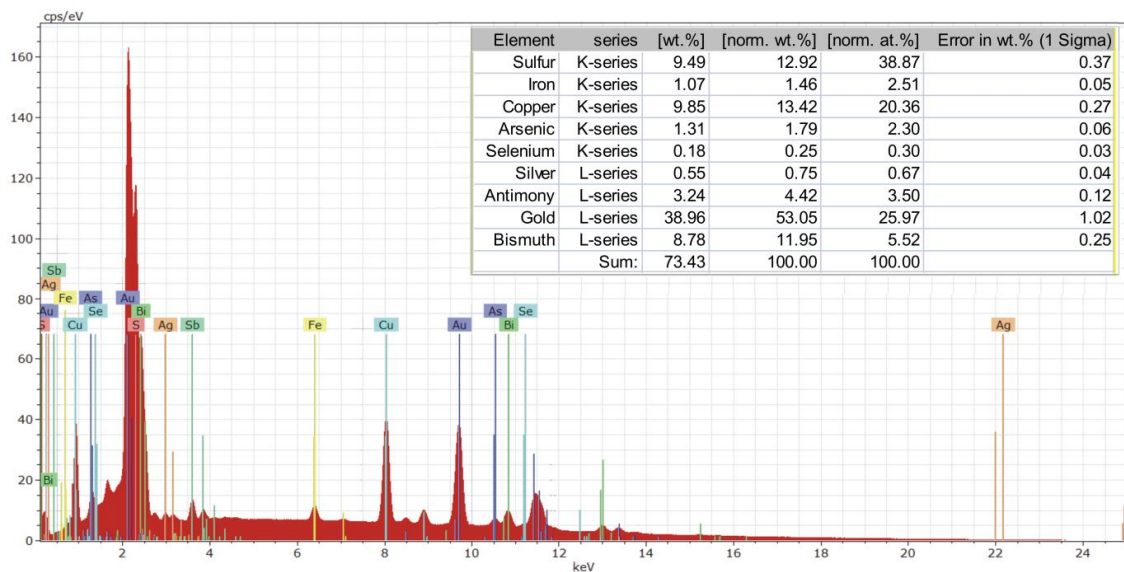


Fig. XV. X-ray spectrum and results of the point analysis Z-11.III – biphasic microinclusion with the elemental composition of covellite-bismuthinite within the Z-11 gold grain

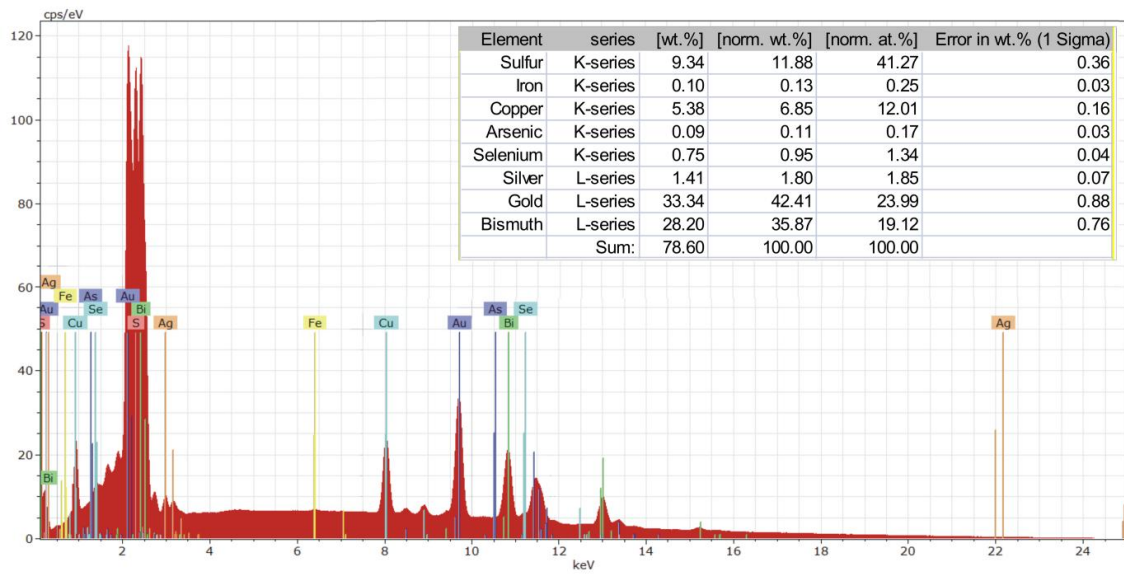


Fig. XVI. X-ray spectrum and results of the point analysis Z-11.IV – biphase microinclusion with the elemental composition of covellite-bismuthinite within the Z-11 gold grain

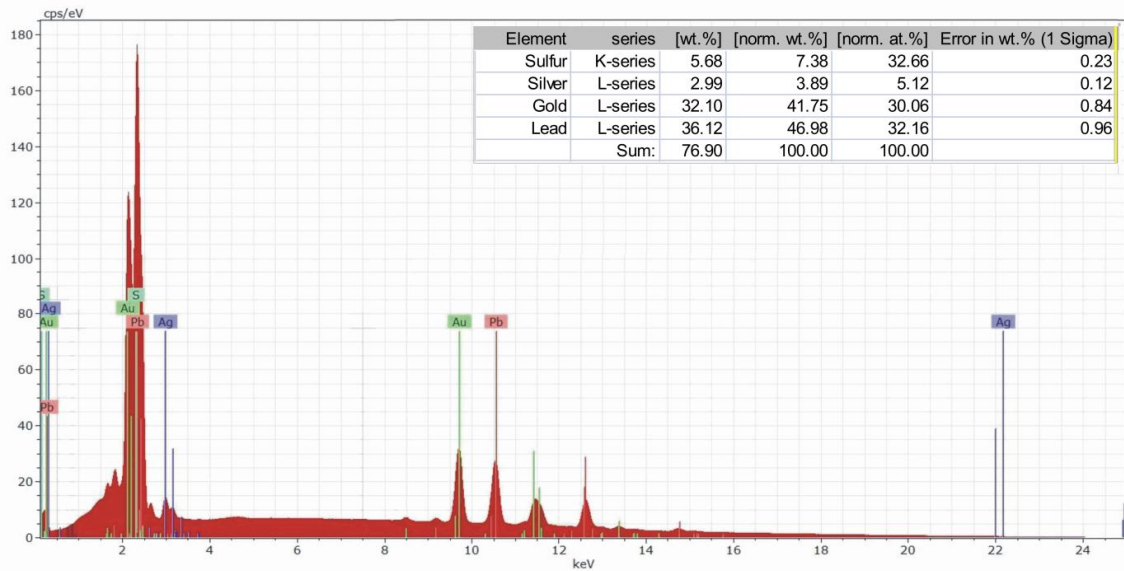


Fig. XVII. X-ray spectrum and results of the point analysis Z-11.V – microinclusion with the elemental composition of galena within the Z-11 gold grain

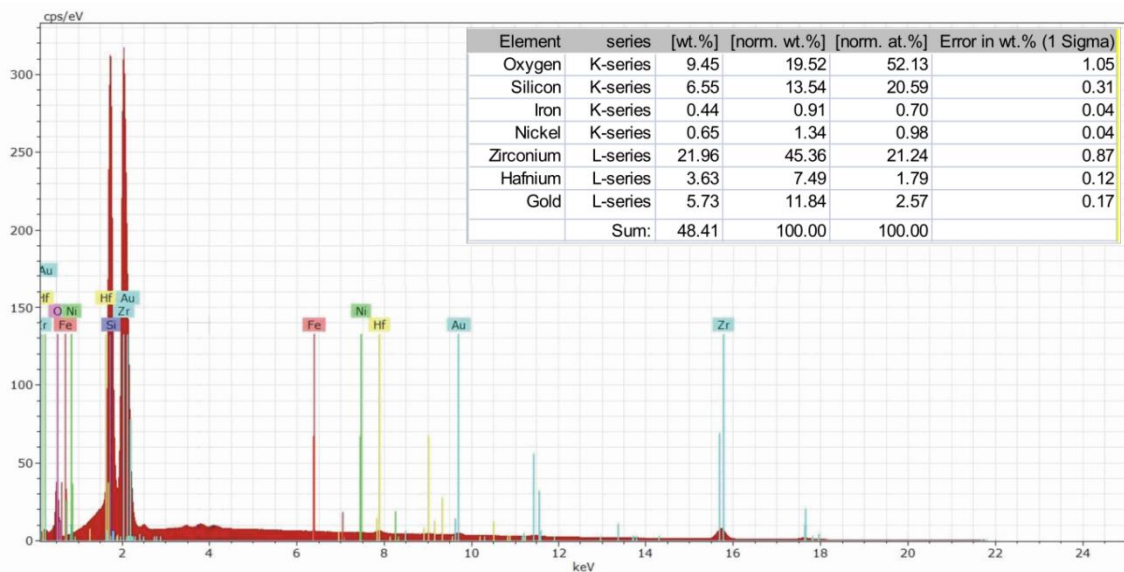


Fig. XVIII. X-ray spectrum and results of the point analysis Z-3.I – zircon within the Z-3 gold grain

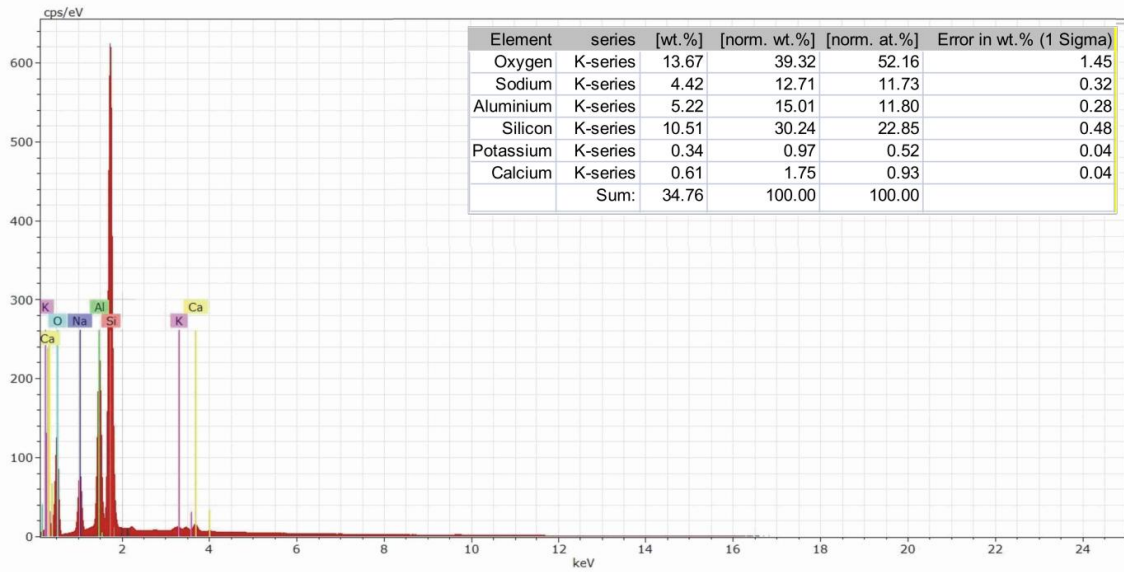


Fig. XIX. X-ray spectrum and results of the point analysis Z-3.II – Na feldspar within the Z-3 gold grain

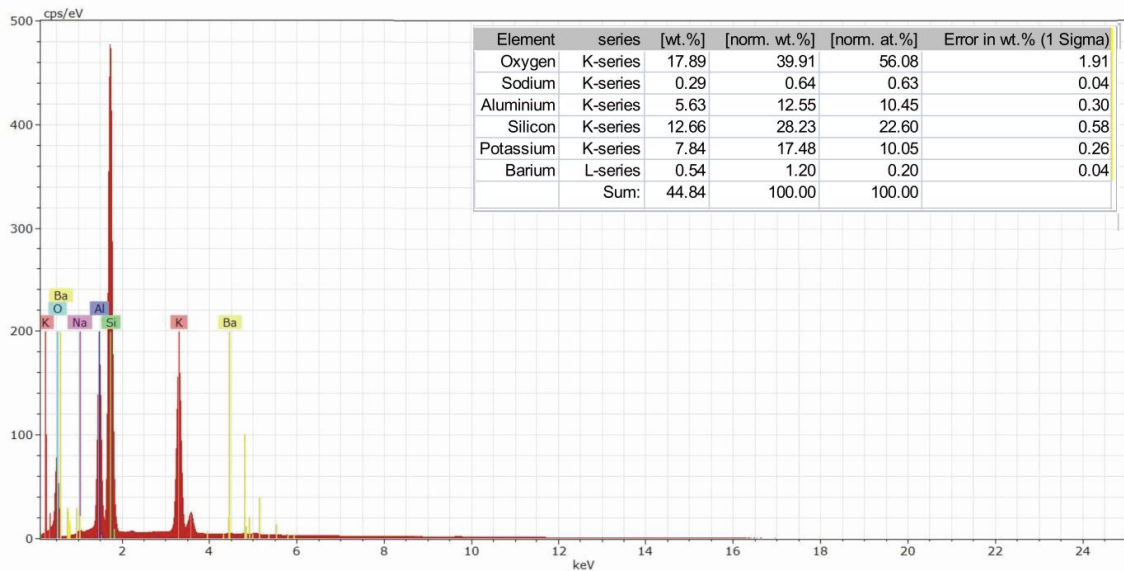


Fig. XX. X-ray spectrum and results of the point analysis Z-3.III – K feldspar within the Z-3 gold grain

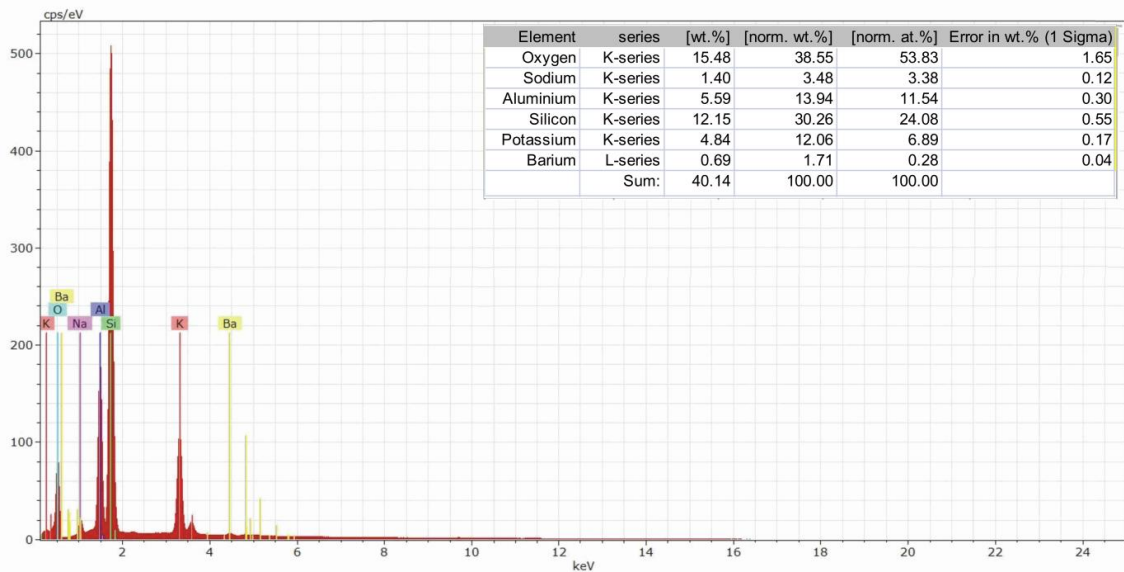


Fig. XXI. X-ray spectrum and results of the point analysis Z-3.IV – K feldspar within the Z-3 gold grain

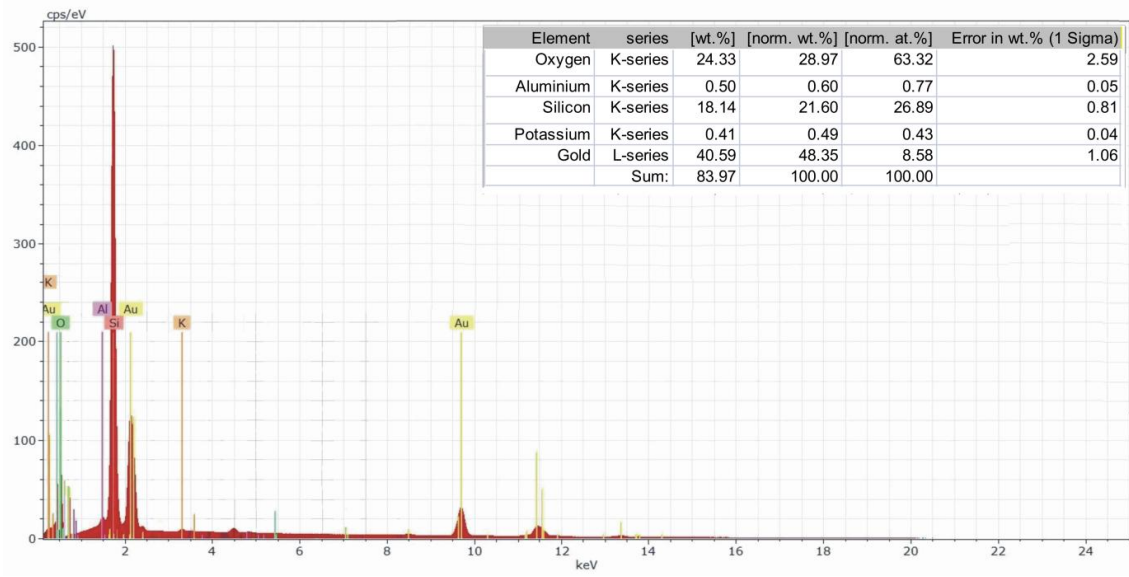


Fig. XXII. X-ray spectrum and results of the point analysis Z-3.V – quartz with microinclusions of native gold within the Z-3 gold grain